

 Open access • Posted Content • DOI:10.1101/2021.03.01.433036

The openCARP Simulation Environment for Cardiac Electrophysiology

— [Source link](#) 

Gernot Plank, Axel Loewe, Aurel Neic, Christoph M. Augustin ...+8 more authors

Institutions: Medical University of Graz, Karlsruhe Institute of Technology, University of Freiburg, University of Graz ...+1 more institutions

Published on: 01 Mar 2021 - bioRxiv (Cold Spring Harbor Laboratory)

Related papers:

- [openCARP: An Open Sustainable Framework for In-Silico Cardiac Electrophysiology Research](#)
- [A demonstration of modularity, reuse, reproducibility, portability and scalability for modeling and simulation of cardiac electrophysiology using Kepler Workflows.](#)
- [A computational framework for cardiac modeling based on distributed computing and web applications](#)
- [Approaching cardiac modeling challenges to computer science with CellML-based web tools](#)
- [Myokit: A simple interface to cardiac cellular electrophysiology](#)

Share this paper:    

View more about this paper here: <https://typeset.io/papers/the-opencarp-simulation-environment-for-cardiac-ya0h1w3rfw>

The *openCARP* Simulation Environment for Cardiac Electrophysiology

Gernot Plank^{1,*#}, Axel Loewe^{2,*#}, Aurel Neic^{3,*#}, Christoph Augustin¹,
Yung-Lin Huang^{4,5}, Matthias A. F. Gsell¹, Elias Karabelas⁶, Mark Nothstein²,
Anton J. Prassl¹, Jorge Sánchez², Gunnar Seemann^{4,5,*#}, Edward J. Vigmond^{7,*#}

¹Gottfried Schatz Research Center, Division of Biophysics, Medical University of Graz, Graz, Austria

²Institute of Biomedical Engineering, Karlsruhe Institute of Technology (KIT), Karlsruhe, Germany

³NumeriCor GmbH, Graz, Austria

⁴Institute for Experimental Cardiovascular Medicine, University Heart Center Freiburg · Bad Krozingen, Medical Center – University of Freiburg, Freiburg, Germany

⁵Faculty of Medicine, University of Freiburg, Freiburg, Germany

⁶Institute of Mathematics and Scientific Computing, University of Graz, Graz, Austria

⁷Liryc Cardiac Modeling Institute, Fondation Bordeaux University, Bordeaux, France

*Corresponding authors: info@opencarp.org

#These authors contributed equally to this work.

Abstract

Background and Objective: Cardiac electrophysiology is a medical specialty with a long and rich tradition of computational modeling. Nevertheless, no community standard for cardiac electrophysiology simulation software has evolved yet. Here, we present the *openCARP* simulation environment as one solution that could foster the needs of large parts of this community.

Methods and Results: *openCARP* and the Python-based *carputils* framework allow developing and sharing simulation pipelines which automate *in silico* experiments including all modeling and simulation steps to increase reproducibility and productivity. The continuously expanding *openCARP* user community is supported by tailored infrastructure. Documentation and training material facilitate access to this complementary research tool for new users. After a brief historic review, this paper summarizes requirements for a high-usability electrophysiology simulator and describes how *openCARP* fulfills them. We introduce the *openCARP* modeling workflow in a multi-scale example of atrial fibrillation simulations on single cell, tissue, organ and body level and finally outline future development potential.

Conclusion: As an open simulator, *openCARP* can advance the computational cardiac electrophysiology field by making state-of-the-art simulations accessible. In combination with the *carputils* framework, it offers a tailored software solution for the scientific community and contributes towards increasing use, transparency, standardization and reproducibility of *in silico* experiments.

1 Introduction

Computational modeling and simulation of cardiac electrophysiology (CEP) has emerged in the last decades and is now playing a pivotal role in basic cardiology research [1]. It also shows high promise as a clinical research tool, for device and drug development [2] and even as a complementary clinical modality, aiding in diagnosis, therapy stratification and planning in future precision cardiology [3]. A key motivation driving CEP model development is the unique ability of providing a mechanistic framework for integrating disparate experimental or clinical data gathered in *in vivo*, *in vitro* or *ex vivo* and subjecting these to thorough quantitative analysis in a matching *in silico* setting. Such *in silico* CEP models allow study of complex cause-effect relationships at a level of quantitative accuracy and biophysical detail beyond what is feasible today with any other research modality.

47 Advanced *in silico* CEP models facilitate the observation of almost any quantity of interest at high spatio-temporal
48 resolutions at scales ranging from cellular to organ, including studies on human hearts, without being limited by
49 ethical constraints. These advantages have led to a marked increase in modeling-based or modeling-augmented
50 publications in cardiology since the early 2000s (Figure 1) with a wide variety of different software implementations,
51 e.g. illustrated in [4–8] or a joint verification benchmark effort of the CEP community [9].

52 Today, simulations of cardiac function in anatomically accurate and biophysically detailed *in silico* models
53 have become feasible. Key factors hampering a further adoption of *in silico* CEP models in advanced application
54 scenarios in basic research, industrial device development and clinical decision making are the limited access to
55 cutting edge simulation technology, and the inherent complexities involved in using such sophisticated tools. These
56 factors render setting up and performing advanced simulation studies a challenging endeavor. In this paper, we
57 present *openCARP*, a CEP modeling environment fully open for academic use that aims to lift these limitations
58 to increase accessibility and, thus, boost adoption of *in silico* analysis of CEP. To cope with the broad range of
59 demands in terms of efficiency, flexibility and usability, the *openCARP* modeling environment comprises two
60 major software components: the actual *openCARP* simulator and an open source Python framework, referred to
61 as *carputils*, for describing *in silico* experiments. *carputils* facilitates building and sharing multiscale workflows
62 by standardization of parameterization, execution, and archiving of simulations, to increase reproducibility and
63 enhance robustness and reliability of complex CEP studies. In general, *carputils* can be adapted to support other
64 CEP simulators as well. Infrastructure supporting interaction combined with extensive tailored documentation and
65 regular user meetings provide the basis for fostering a vibrant user community.

66 This paper first gives a brief historic overview of the field of CEP simulation software, from the early pioneering
67 days to the current situation that motivated the development of the *openCARP* simulator and *carputils*. Then,
68 we review requirements for a CEP simulation environment to accommodate the needs of a wide user base. We
69 introduce the *openCARP* CEP simulator and the *carputils* Python framework, together with pre- and post-processing
70 components. The use of these tools is described along a typical workflow for setting up a state-of-the-art *in silico*
71 simulation study, that spans from single cell to organ level, covering a wide range of user needs in the CEP modeling
72 and simulation field.

73 1.1 Historical CEP Software Development

74 It was not before the mid-1980s that computational models for studying bioelectrical activity at the tissue level
75 emerged [10, 11]. Unlike modeling work focused on vascular mechanics or hemodynamics, for which – owing to
76 close similarities to applications of industrial relevance – commercial software became available early on, this was
77 not the case for CEP modeling. In the absence of such software, academia had to develop CEP modeling solutions,
78 which has remained that way up until today. While commercially available multiphysics simulators may have CEP
79 modules, they are limited in terms of speed and capability [12]. In general, these do not meet the demands of
80 state-of-the-art CEP studies

81 which have undergone a marked transformation over the past decade, leading to a dramatic increase in
82 complexity [13, 14].

83 As a consequence, the vast majority of published CEP modeling studies have relied on academic in-house
84 codes [15–23]. These software packages have been largely developed by individual laboratories as side projects in
85 support of their applied research work, typically focused on understanding mechanisms underlying the formation
86 and maintenance of arrhythmias [24, 25] and their therapies [26–28]. The direction of software development

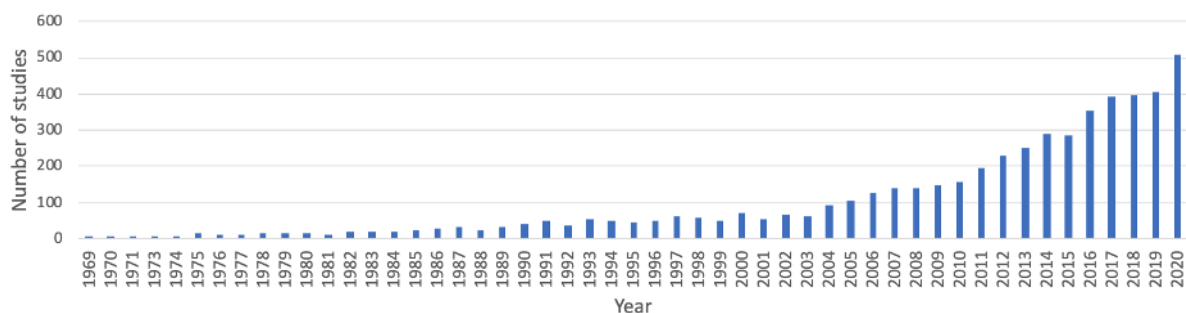


Figure 1: PubMed-listed studies with “(atria* OR ventric* OR cardi*) AND (“computer model” OR “mathematical model” OR “computational model” OR “in silico”)” in title or abstract.

87 has been largely steered by the needs of funded projects. Often, this led to *ad-hoc* development processes
88 yielding research prototypes but no sustainable software products for long-term use, rather than a roadmap-based
89 development targeting longer term strategic goals. Moreover, particularly during the pioneering years, the modeling
90 infrastructure encoded the specific expertise of individual labs. Sharing of software or models across labs was
91 uncommon. Research on CEP resulting in discovery has been traditionally regarded as being of higher academic
92 merit than research on building the enabling CEP modeling methodology, which requires a similar amount of
93 human resources. Thus, modeling has been significantly less well funded, which has opened a gap between the
94 often highly ambitious scientific goals and the available technical capabilities [29].

95 For at least the first three decades of CEP modeling, the single lab paradigm was the prevailing approach in the
96 development of CEP modeling infrastructure. An important factor rendering this approach viable was the simple
97 nature of CEP simulations during these early years, making it feasible for a single graduate student to develop and
98 write code for the problem at hand. Models of cellular dynamics were relatively simple [30–32], and geometric
99 representations were anatomical abstractions, comprising 1D strands, 2D sheets or, later in the late nineties when
100 computational resources became more powerful, 3D slab or wedge preparations. These regular domains lent
101 themselves quite naturally to simpler spatial discretization techniques, with the finite difference method (FDM)
102 appropriate for the vast majority of studies. Numerical techniques were less well developed and much simpler to
103 implement, or generic implementations made available as numerical libraries were integrated.

104 **1.2 Current State of CEP Modeling**

105 Over the past decade though, the complexity of CEP simulations has increased exponentially as the result of several
106 factors:

- 107 i) faster, and higher resolution tomographic imaging modalities
- 108 ii) an explosion of biological knowledge leading to more components in cell models, as well as more complicated
109 formal descriptions of these components and interactions between them
- 110 iii) more elaborate numerical methods which improve performance at the cost of increased complexity
- 111 iv) evolving computer architectures which demand specific data layouts and algorithms to fully exploit the
112 resources

113 Complexity has increased beyond the capabilities of a single lab development paradigm.

114 State-of-the-art modeling studies use unstructured, high resolution, image-based tomographic reconstructions
115 to reflect individual cardiac anatomies with high geometric fidelity and avoid spurious boundary artefacts introduced
116 by jagged surfaces of Cartesian grids. Unstructured tessellation has prompted more sophisticated discretization
117 techniques, such as the finite element method (FEM) [33] or the finite volume method (FVM) [34], which are
118 substantially more costly to implement and time-consuming to develop a profound understanding of. CEP is
119 studied at the organ scale in biventricular or biatrial models and recently models representing all chambers of the
120 heart are beginning to be used [35].

121 Such four chamber models account for anisotropic tissue properties and discrete conduction pathways in all
122 chambers, the specialized cardiac conduction system comprising sinus node [36–38], atrio-ventricular node [39]
123 and the His-Purkinje system [40]. Pathologies altering conduction velocities or pathways such as ischemia [41],
124 infarct scars and surrounding transitional tissue [42], or various types of fibrotic lesions [43–45] are considered at
125 increasing levels of physiological [46] and structural detail [47–50].

126 Along with the structural heterogeneity, a large number of cellular models are needed to account for functional
127 heterogeneity across different regions of the heart, often with subtle variations within regions to account for
128 gradients in protein expression that alter action potential (AP) morphology. The *CellML* markup language, along
129 with its repository (cellml.org), was created to aid in the standardization and dissemination of these models [51].
130 Beyond the numerous issues in developing the software, major challenges in building *in silico* experiments have
131 to be addressed. Sophisticated workflows have been conceived to facilitate automated translation of segmented
132 image data sets into discrete meshes suitable for simulations [52–54]. These workflows are constantly refined to
133 render the production of increasingly larger numbers of individualized models, often referred to as *virtual cohorts*,
134 feasible [35]. In the process of functional personalization of such models, tuning parameters have to be identified
135 to achieve a close fit with observed data. Experimental or clinical protocols are mimicked *in silico* to match *in*
136 *vivo* experiments or clinical conditions ever more closely. These procedures typically require simulating prolonged
137 periods to ensure convergence to a limit cycle, and the number of simulations executed within optimization loops
138 tend to be high. Overall, these factors, in combination with the numerical demands imposed by CEP – the fast
139 upstroke of the action potential translates into depolarization wave fronts of limited spatial extent (<1 mm) – render
140 the execution of modeling studies a challenging endeavour. Such studies can only be executed with highly efficient,

141 robust and versatile CEP simulation tools. The costs in terms of personnel necessary to develop such tools from
142 scratch is daunting. For instance, the cost of development of *CARP*, the proprietary predecessor of *openCARP*,
143 is estimated to be around 50 person-years, not including any of the pre- and post-processing codes necessary for
144 building the workflows.

145 1.3 Towards a Common Software

146 In other fields, certain software has been adopted by a critical mass of the community and thus have become the
147 *de facto* standard for the entire field. Examples of this are *Neuron* for neural simulation [55], and *GAMESS* for
148 chemistry [56]. While the need for standardized, open software has been recognized before within the CEP modeling
149 community, no software has achieved such a status. Preceding initiatives in this vein include *openCMISS* [18] and
150 *Chaste* [57], but their success has been mixed so far, as their rate of adoption has been rather marginal. Reasons are
151 multifactorial: For groups developing numerical methods, there is limited demand as they have the capability to
152 build custom tailored frameworks themselves [23, 58–62] that facilitate the implementation of disruptive changes
153 at any time, without the frictional losses involved in community projects where changes have to be agreed upon
154 by various stakeholders. This is in stark contrast to the demands within the applied CEP modeling community.
155 A broad web-based survey conducted by us in 2017 showed that for a convergence in the CEP field, simulation
156 environments are needed which meet most or, ideally, all of the following requirements:

- 157 • **Feature completeness**, i.e. a simulator should have the features to be able to replicate a large share of
158 published modeling studies using other software [57, 63]. It must be able to perform the functions of any
159 software it is replacing, as well as offer new functionality.
- 160 • The simulator needs to be made **available** under a license that allows unrestricted academic use [64].
- 161 • A **streamlined installation** process for all popular deployment targets without the need to deal with intricate
162 technical challenges of compilation and software dependencies [64].
- 163 • An intuitive and flexible **user interface** that exposes input parameters in an intuitive way while accom-
164 modating a wide range of experimental conditions and protocols. Consistent interfaces are the basis for a
165 positive and intuitive user experience [65].
- 166 • Comprehensive **user documentation** for all tools, combined with **extensive training material**, such as
167 tutorials for all simulator features to get new users started within a reasonable time, and a tractable learning
168 curve [64].
- 169 • The simulation environment should provide streamlined, **standardized workflows** to share, reproduce, and
170 archive *in silico* experiments [66]. It should be easy to export results, together with all relevant input data,
171 in one bundle. A high degree of standardization also facilitates the sharing of expertise between groups.
- 172 • A vibrant **user and developer community** is key for a sustainable research software [67]. These communities
173 should be supported by interactive platforms, spur development (feature requests, bug reports), and interact
174 via webcasts and user meetings [64].
- 175 • The simulator should be **computationally efficient** on all common hardware platforms ranging from local
176 workstations to national high performance computing facilities [68].
- 177 • **Code documentation** with a thorough description of classes, methods and interfaces, as well as the overall
178 software architecture, lowers the barrier for users becoming developers and contributing to the project.
179 This documentation, in combination with a modular and extensible architecture, is the basis for sustainable
180 research software [69].
- 181 • Import from (e.g. *CellML* [51] for cellular models) and export to (e.g. VTK [70]) common data formats
182 increases **interoperability**. Easy integration in existing pre- and post-processing workflows attracts a wider
183 range of users. The version of the simulator code used to generate a result should be clearly identified and
184 accessible via a persistent and citable identifier.
- 185 • A high level of trust in the correctness of the software implementation is instrumental. The functionality of
186 the simulator needs to be verified and constantly controlled by **quality assurance** measures. Before entering
187 the master branch, new code should be reviewed by maintainers. Test cases should cover all use cases and
188 be executed for each build before deployment [64]. The necessary trust is best established in a positive
189 feedback loop wherein a critical mass of CEP modeling labs adopts and successfully uses the software for a
190 broad range of modeling applications over prolonged periods.

191 2 Methods and Results

192 The main objective of the *openCARP* initiative is to provide and establish simulation software within the CEP
193 modeling community which fulfills the criteria outlined above. To better meet these user requirements, the
194 *openCARP* modeling environment is organized as comprising two major software bundles, the actual code for
195 executing simulations, i.e., the *openCARP simulator*, and a framework for describing *in silico* experiments, referred
196 to as *carputils* (Fig. 2). The *openCARP* simulator has been developed with the following objectives in mind:

- 197 • **Accessibility:** The main distribution mechanism of *openCARP* emphasizes binary packaging for commonly
198 used platforms (currently Linux and macOS), platform-independent Docker containers, and a detailed
199 documentation supporting source installations on all levels of computers including large-scale national
200 HPCs. Only providing a source installation excludes major parts of the user community who are not
201 sufficiently versed in compiling scientific software, or do not want to manage a complex software stack,
202 especially given the release requirements and potential conflicts with compilers and underlying software
203 libraries. The source code of all *openCARP* components is maintained in the public GitLab instance
204 git.opencarp.org. *carputils* is published under the Apache 2.0 open source license, and the *openCARP*
205 simulator under the [Academic Public License](#) restricting the open use to academic non-profit cases. A
206 commercial license can be requested.
- 207 • **Interoperability:** *openCARP* builds on two decades of CEP modeling experience gained with its proprietary
208 predecessors, *CARP* [16] and *acCELLerate* [17], with a stable user base about 130 registered users. The
209 predecessor software packages have been extensively used by several CEP modeling groups and led to
210 >250 peer-reviewed journal publications, covering the full range of modeling issues including numerical
211 methods [71], anatomical modeling and model functionalization [48, 72] as well as a broad range of
212 applications such as formation and maintenance of arrhythmias [73, 74], EP therapies [75, 76], diagnostic [77,
213 78] and therapeutic applications [79, 80]. The *openCARP* simulator has been built from scratch in terms of
214 code, but the user interface is consistent with previous proprietary versions of *CARP* [16] to facilitate re-use
215 of a large number of existing experiments. Moreover, *openCARP* interoperates with relevant community
216 standards by providing input and output interfaces VTK [70] and *CellML* [51], for example, either directly or
217 via other tools. All *openCARP* specific formats and standards are openly available and concisely described,
218 with adequate tools for their management provided as source code.
- 219 • **Performance:** *openCARP* has been implemented from scratch in C++ (2011 standard) but follows the same
220 discretization and solver schemes that have been used successfully in the predecessor code *CARP* [16, 71].
221 Briefly, the *openCARP* simulator spatially discretizes the partial differential equations underlying the mono-
222 or bidomain model (or potentially other physics like mechanics) using the FEM [81, 82] with linear basis
223 functions. The bidomain equations are cast in the elliptic-parabolic form and decoupled to be solved
224 sequentially [83], with various time stepping options including fully explicit Euler or θ -schemes, with or
225 without operator splitting, leading to fully explicit or implicit-explicit solver schemes as the reaction term
226 is always treated explicitly. The interested reader is referred to the *openCARP* user manual for numerical
227 details. The FEM implementation makes use of parallel mesh management and mesh partitioning [68].
228 The resulting linear systems of equations are solved with *PETSc* [84], with various pre-configured solver
229 options [85–87], under exploitation of parallel algebraic matrix-vector operations, parallel I/O, and timing
230 routines among others. On each node, the embarrassingly parallel *LIMPET* library [88] is used to calculate
231 the cellular electrophysiology models. Time integration schemes for these ODE systems can be controlled
232 per variable and include Runge-Kutta, Rush-Larsen, Rosenbrock [89] and advanced schemes accessible via
233 *CVODE* [90] with adaptive step size and error control. While profiling and benchmarking plays a central role
234 during development, *openCARP* does not yet employ detailed benchmarking or profiling during integration
235 testing. Currently, integration tests are binned into different execution time groups and tests changing group
236 are marked as failed.
- 237 • **Transparency:** The availability as source code will benefit the technically affine model developers in
238 the CEP modeling community by allowing implementation of additional features, the critical revision of
239 numerical schemes, and the identification of weaknesses. This will trigger constant re-engineering of
240 the software and, thus, help improve software quality. The software is version controlled using git and
241 connected to continuous integration / continuous delivery (CI/CD) services with integration testing of most
242 simulation setups (currently 74 individual simulations). We have opted against unit testing at the current
243 stage of development. Release versions of *openCARP* [91] are automatically archived and uploaded to
244 the RADAR4KIT repository as part of the continuous deployment pipelines [92]. Submission information
245 packages are built in BagIt format and comprise the source code, the binary versions for the support
246 platforms, the respective version of the documentation and test reports. Metadata is automatically extracted

247 from machine-readable files in the git repositories and provided according to the DataCite 4.3 scheme [93].
248 A DOI is minted for all published and archived versions to ensure long-term accessibility.

249 *carputils* is a framework designed to define and execute *in silico* experiments by encoding the complex
250 workflows of advanced CEP simulation studies in a reasonably standardized manner. By providing an additional
251 abstraction layer on top of the *openCARP* simulator itself, we aim to achieve the following objectives:

- 252 • **Usability:** The main focus of *carputils* is on providing a modeling and simulation environment which
253 enables researchers to carry out a wide range of studies out of the box. Only a physiological understanding
254 of the problem at hand should be necessary for executing such experiments, not knowledge of underlying
255 numerical details.
- 256 • **Reducing complexity:** *In silico* experiments defined with *carputils* facilitate learning by exposing only a
257 small number of relevant parameters which are needed for controlling a given experiment.
- 258 • **Reproducibility:** By providing mechanisms for easy sharing of *in silico* experiments, *carputils* contributes
259 to the concept of Open Science and facilitates reproducibility and reuse. Owing to the complexity of
260 experiments, the ability to share them has been severely hampered, even within the same laboratory, let
261 alone across different ones. We overcome barriers posed by numerous differences in local installations,
262 inconsistencies between code revisions, and the management of high dimensional input parameter spaces
263 defining a setup: meshes, label fields, electrode definitions and pacing protocols, limit cycle state vectors,
264 structural entities such as fibrotic lesions or scars, functional heterogeneities, conduction system topology,
265 and parabolic solver method, to name but a few important ones.
- 266 • **Productivity:** *carputils* aims to boost productivity by providing standardized workflows for common tasks
267 such as setting conduction velocities, computing limit cycles of ionic models to generate initial states,
268 interrogate restitution properties, or post-processing and visualization of outputs.
- 269 • **Abstraction:** *carputils* uncouples technicalities of executing simulations on different platforms from ex-
270 periment design such that they can be executed on any supported platform – from laptops to national HPC
271 facilities – using the exact same command line. Platform-specific aspects related to scheduling and launch-
272 ing of jobs are hidden from the user, and encapsulated in abstract platform descriptions. Only generic user
273 choices such as the number of processes to be used in a simulation must be provided.
- 274 • **Quality assurance:** Support for **regression testing** of all major simulator features is built in, including
275 automated nightly building and testing of the entire software stack. *carputils* encodes a range of **verification**
276 **benchmarks** such as the CEP N-version benchmark [9] and a suite of additional performance benchmarks
277 of varying level of complexity, ranging from biventricular slices up to whole heart models, for measuring
278 simulator performance, or for investigating the effect of numerical settings.

279 Additional open source software components have been developed to support the modeling, simulation and
280 visualization when using *openCARP* as shown in Fig. 2. *meshtool* [54] (License: GPL v3) allows generating or
281 interacting with geometric data. *carputilsGUI* (License: Apache 2.0) is a web-based graphical user interface to
282 control specific *carputils* experiments and visualize results within the browser for low-threshold entry to *openCARP*.
283 *meshalyzer* (License: GPL v3) is a tailored visualization program for CEP, even though VTK export allows seamless
284 visualization in *ParaView* [94] as well.

285 *openCARP* provides documentation for users with different levels of experience. [Video tutorials](#) introduce users
286 to the basics of CEP modelling and guide them through their first steps with *openCARP*. Further videos introduce
287 standard simulation pipelines and progressively advanced features covering the whole gamut from single cell
288 simulations to 3D heart models including pre- and post-processing steps using the *carputils* framework. [carputils](#)
289 [examples](#) cover common simulation scenarios and provide a starting point to develop custom *carputils* experiments
290 in combination with the [API documentation](#). The *openCARP* [reference documentation](#) contains all *openCARP*
291 parameters to give full control of all aspects. Continuous deployment pipelines ensure that documentation (web
292 page, PDF) is always in sync with the code by automatically generating these artifacts based on the code.

293 2.1 Workflows and Use Cases

294 In the following sections, we introduce the *openCARP* simulation framework by covering common workflows
295 for use cases ranging from the cellular to the organ level. Specifically, we elucidate the key processing steps
296 to implement a human biatrial model of persistent atrial fibrillation. An overview of a standardized processing
297 workflow is given in Fig. 3.

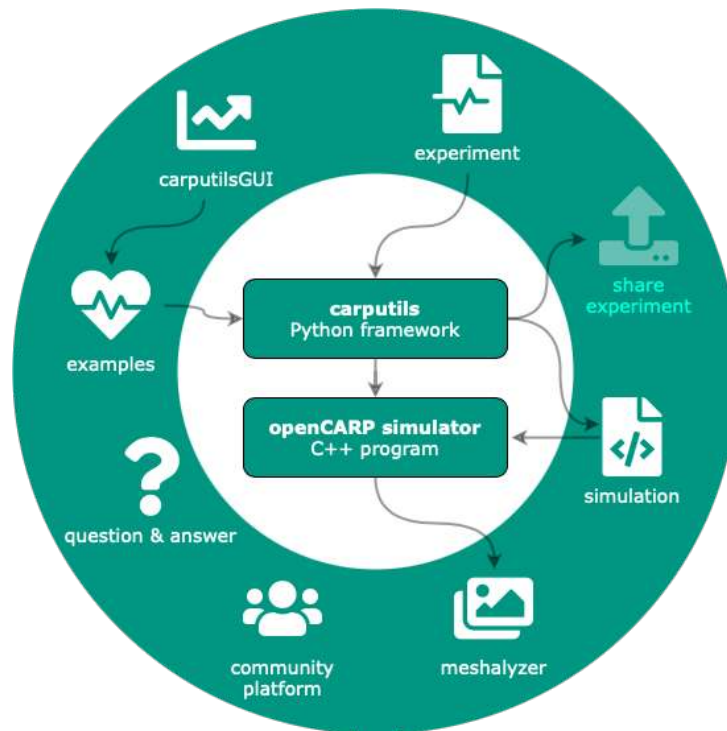


Figure 2: The *openCARP* ecosystem comprises several components that interact with its central pillars: *carputils* and the *openCARP* simulator. Users can write their own experiments using the *carputils* Python framework, or start with existing *examples*. *carputils* will set up the simulation, launch the *openCARP* simulator, perform postprocessing steps and call *meshalyzer* for visualization. Apart from the commandline interface, *examples* can also be parametrized, run and visualized using the web-based *carputilsGUI*. A community platform including a question & answer system completes the *openCARP* ecosystem.

298 2.1.1 Cellular Level

299 The ordinary differential equation (ODE) models representing cellular dynamics and ion current across the mem-
 300 brane are integrated in the *LIMPET* library. *openCARP* is shipped with a set of commonly used models (including
 301 Courtemanche et al. [98] Koivumäki et al. [99], ten Tusscher et al. [100], O’Hara et al. [101]). The commandline
 302 tool *bench* is an interface for carrying out single cell experiments to tune models of cellular dynamics to given
 303 (patho-) physiological conditions. The most basic use case is to compute APs for a given membrane model.
 304 Advanced features of *bench* are to control stimulation, compute restitution curves under various protocols, to carry
 305 out voltage clamp experiments or to clamp arbitrary other state variables.

306 `bench --imp=Courtemanche --clamp-SVs=Ca_i --SV-clamp-files=Cai.dat`

307 for example would clamp the intracellular calcium concentration of the Courtemanche et al. model to the time
 308 course defined in the `Cai.dat` file. The output files can either be processed with custom scripts or, ideally, pre-
 309 and postprocessing is integrated into a *carputils* Python script encoding the entire experiment including the call
 310 to *bench*. Besides CEP models, *bench* also provides myofilament models of active tension development. Often,
 311 one wants to change parameters of the cellular model to investigate how changes to a model component, due to
 312 e.g. drug effects, genetic mutations or disease-induced remodeling, affects behaviour. Parameters can easily be
 313 adjusted in *LIMPET* by specifying a value directly, or by using mathematical operations to alter the value relative
 314 to the default.

315 `bench --imp=COURTEMANCHE`
 316 `--imp-par="Gto-65%, GK1*2, GKs*2, GKur-50%, GCaL-55%, maxI_NaCa+60%, maxCa_up*0.5, C_m+20%"`

317 for example would adjust the Courtemanche et al. model to reflect conditions of persistent atrial fibrillation-induced
 318 remodeling of cellular CEP [102] (Figure 4). The models equations are encoded in *EasyML*, a markup language
 319 developed for human readability. Changes to the model structure or parameters that are not exposed by default

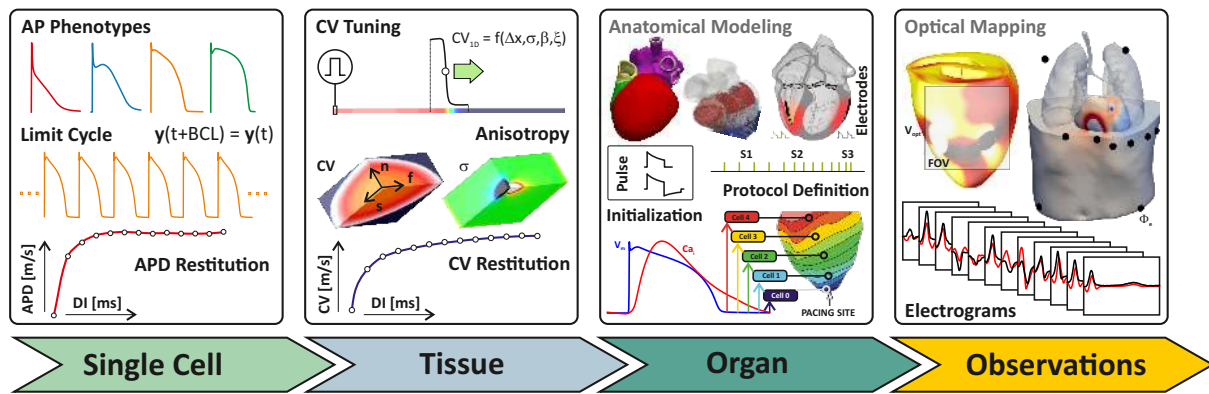


Figure 3: Overview of typical steps in an advanced CEP simulation study. **Single Cell:** AP phenotypes of different types of tissues are defined, paced to a stable limit cycle for a given set of cycle lengths, and dynamic properties such as APD restitution are evaluated. Initial state vectors y_0 are stored for each phenotype. **Tissue:** Conductivities σ_ζ are determined for the mean spatial resolution Δx of the organ-scale mesh, given surface-to-volume ratio, β , and numerical settings, ξ , by simulating uniform wavefront propagation in 1D along an eigenaxis, ζ , to obtain the desired CVs along fiber, f , sheet, s , and sheet-normal, n , direction, and anisotropy ratios between intra- and extracellular domain. CV restitution is evaluated then by measuring CV under increasingly shorter diastolic intervals. **Organ:** Organ models are generated using anatomical modeling pipelines, currently not included in *openCARP*, consisting of mesh generation, definition of fiber architecture, labeling of regions, computation of anatomical reference frames [95–97] and possibly the incorporation of a cardiac conduction system. Location and geometry of electrodes is defined, as are the pulse shapes used for stimulation and the pacing protocol. The organ model is then populated by assigning the ionic model initial states y_0 , as computed for each phenotype, to the respective tissues, and conductivities are assigned to the various regions to control CV. A pre-pacing protocol is applied to ascertain that the organ-scale model is as close as possible to a limit cycle for the given cycle length. **Observations:** Additional model components are set up to simulate observable data such as optical transmembrane voltages, V_{opt} , invasively recorded electrograms Φ_e , and non-invasive ECGs recorded from the body surface.

320 can easily be implemented in the `.model` files directly. An automated way to produce shared libraries that can
 321 be loaded at run time allows using these custom-built models or adapt numerical time integration without having
 322 to recompile the entire simulator. Additional models can be included using *CellML*, the XML-based community
 323 standard for ionic models. Models downloaded from the *CellML* repository [51] can be converted to *EasyML* using
 324 [tailored commandline scripts](#) or interactively via the third-party tool *Myokit* [103].

325 Initial conditions for tissue scale simulations are generated with *bench* by creating a set of myocyte models
 326 representing the CEP heterogeneity at the tissue scale. Each myocyte model is paced at one or more basic cycle
 327 lengths based on the activation rates desired for the tissue model until the model settles in to a limit cycle. Initial
 328 state vectors of each myocyte model are stored, to be used later to populate the tissue and organ scale model as
 329 detailed in the [limit cycle initialization example](#). Tailored experiments for interrogating and tuning of dynamic
 330 properties of ionic models such as [APD restitution](#) are also provided.

331 2.1.2 Simple Tissue Level

332 Simple geometries allow investigating fundamental mechanisms and determining properties of tissue CEP. These
 333 simple geometries play an important role in the generation and interpretation of modeling results as one can
 334 investigate basic mechanisms by isolating the effects of confounding factors, such as the prevailing myocyte
 335 orientation (“fiber orientation”) or geometric complexities. Additionally, tissue behavioural properties can be
 336 quantified easily from these simplified models.

337 Mesh resolution has to strike a balance between computational effort and numerical accuracy. We refer to the
 338 N-version monodomain benchmark for spatial convergence considerations [9]. Tissue and cellular level properties
 339 need tuning to replicate activation and repolarization sequences as observed in wet lab experiments or the clinic.

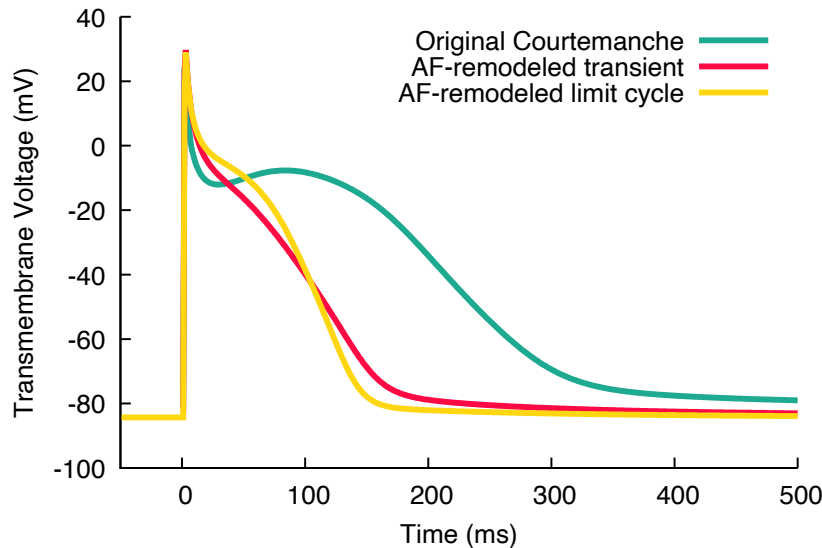


Figure 4: Action potentials of the original Courtemanche et al. [98] model (green) and remodelled variants reflecting persistent atrial fibrillation (AF) conditions [102]. Red: first action potential with the adapted parameters and initial state of the original model. Yellow: limit cycle AP after transient changes of the diastolic state equilibrated (100 stimuli at a basic cycle length of 1 s).

340 Stimulation patterns initiate propagation with a velocity which varies as a function of space. The anisotropic CV is
341 determined by myocyte orientation, the tissue conductivities along and across the myocytes, the surface-to-volume
342 ratio, and the fast sodium current of the cells, but modified by the curvature of the activation wavefront, and the
343 refractory state of the sodium channels. Technical factors related to spatial discretization and time integration also
344 play a role, particularly when using coarser spatial resolutions [9]. Specifically, the tissue conductivities need to
345 be determined to ensure physiological direction-dependent CVs before running more complex simulations. This
346 is easily performed using the *carputils* tool *tuneCV* [104]. A wave front propagation in a 1D strand is simulated
347 using the desired AP phenotype, and the CV measured at the center of the strand for given numerical settings and
348 spatial resolution. Thus, *tuneCV* compensates for artificial alterations in CV due to grid spacing, which is chosen to
349 balance numerical accuracy and computational cost [9]. A comprehensive introduction to *tuneCV* can be found in
350 the *carputils* example “Tuning Conduction Velocity”. Other tissue properties like effective refractory period (ERP),
351 vulnerable window or alternans can also be easily investigated in simple 1D geometries, for example, to extract
352 arrhythmia predictors [28]. Additionally, rate dependent changes (restitution) of parameters provide insight into
353 tissue behavior at fibrillatory activation rates. CV restitution is for example investigated in the *carputils* example
354 “CV Restitution”.

355 Simple 2D geometries can be used, for example, to investigate the effects of spatially heterogeneous tissue
356 properties on arrhythmia dynamics. Spatial AP heterogeneity plays an important role in CEP as key features such as
357 excitability, AP morphology and duration vary throughout the heart. Numerous effects of clinical relevance cannot
358 be explained under the assumption of homogeneous tissue properties. Important examples are naturally existing
359 heterogeneities within the ventricle that are responsible for the concordant T-wave in the ECG [105] and spatial
360 changes of tissue conductivity (e.g. due to fibrosis) or/and electrophysiological properties in atrial fibrillation.
361 In CEP modeling, two different approaches exist to account for spatial heterogeneity: either distinct regions are
362 identified in which properties are uniform, or functions of space are defined which describe parameter variation,
363 with granularity only being limited by spatial resolution. Region-based definition is, in general, easier to manage,
364 but generates abrupt changes across region boundaries which may lead to behavioural artifacts. Function-based
365 assignment is more flexible and facilitates smooth variations that avoid potentially artificial high gradients, but is
366 more challenging to define, particularly for complex anatomical models that, typically, require auxiliary anatomical
367 coordinate systems to impose a desired variation [95–97]. The *carputils* example “EP Heterogeneity” illustrated
368 the use of region-based heterogeneities, with four regions in which parameters can be set differently. Fig. 5A shows
369 the impact of region-based variation in excitability upon the activation pattern. A comparison between region and
370 gradient based heterogeneity is shown in another *carputils* example.

371 Key advantages of *in silico* CEP models over *in vivo*, *ex vivo*, or *in vitro* models are their ability to precisely
372 control all parameters, to observe all quantities of interest at high spatiotemporal resolution, to test large parameter

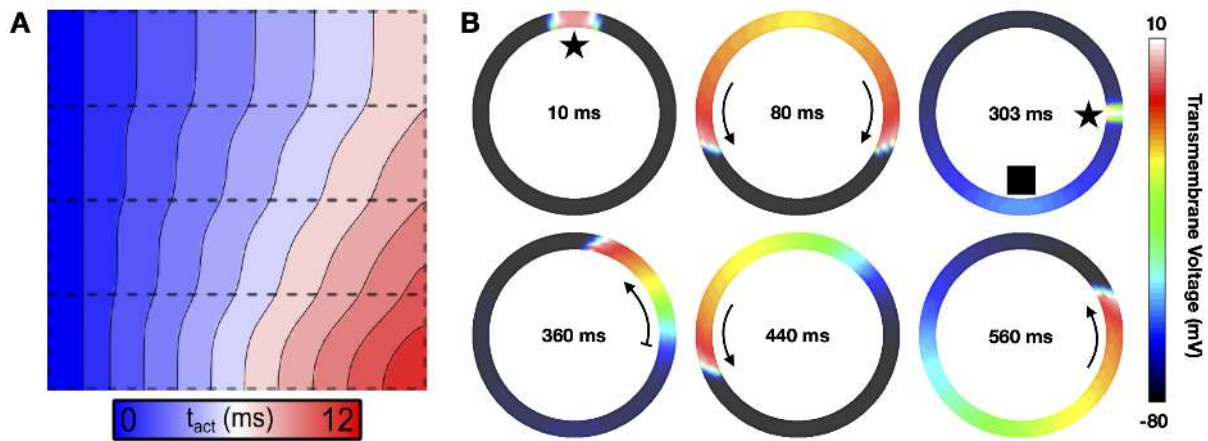


Figure 5: A: Activation times (t_{act}) in a model with four regions of varying excitability. From the bottom to the top region, the conductance of the fast sodium channel (g_{Na}) is set to 1x, 2x, 4x, and 8x g_{Na} of the nominal value, respectively. Planar wave fronts initiated along the left edge of the sheet gradually distort due to these differences in CV. B: Initiation of a rotating wave in a ring model in a stylized representation of an atrial slice. The initial stimulus (delivered at 10 ms, marked by a star) induces bidirectional propagation (80 ms). At the end of the refractory period (303 ms), a second stimulus delivered at a different site located at a critical recovery isline initiates a wave front that is blocked from propagating downwards where tissue is still refractory (rectangle). This leads to unidirectional propagation upwards (360 ms), setting up a sustained anatomical reentrant activation pattern (440 ms and 560 ms). This simulation was performed with ionic model settings corresponding to the persistent atrial fibrillation variant of the Courtemanche et al. model referred to above. In a healthy model, reentry cannot persist as the wavelength is too large for the given ring dimension.

spaces in a reproducible fashion, without being restricted by ethical concerns. Thus, mechanisms underlying CEP phenomena such as the formation and maintenance of an arrhythmia can be dissected in detail under a wide range of experimental settings. While organ-scale models are most comprehensive as they represent all factors at play, simplified 2D models are also highly relevant as these can provide crucial mechanistic insights with fewer confounding factors. Owing to their lighter weight, large parameter spaces can be probed and the observation of key variables and phenomena is more easily achieved than with the larger organ-scale models. Ring models representing a slice across a single cardiac chamber are a simple and popular 2D geometry for studying macro-reentrant arrhythmias. Fig. 5B illustrates the induction process of a reentrant wave in such a model. Reentrant activation is only sustained if the wavelength, defined as $CV \times ERP$, is shorter than the perimeter of the ring. 2D sheet models can also be used to trace functional reentries, but their induction is less simple compared to the ring. The *carputils* example “Induction Protocols” presents four different methods to induce reentry in a sheet.

2.1.3 Organ Level

For whole chamber or organ level models, meshes must be created that accurately reflect the anatomy of the entity to be modelled. Streamlined workflows for this task are currently under development by various labs [106], typically relying on connecting heterogeneous software components, including commercial software, that are specialized for particular processing stages, ranging from multi-label segmentation, meshing, fiber architecture generation [107], anatomical reference frame generation [95–97] or topology generation of the specialized cardiac conduction system [108]. The Python-based *carputils* is perfectly suitable for creating such workflows [109]. However, owing to the technological heterogeneity of all this software, a complete integrated workflow is currently not available within *carputils*, but many basic elements required for building such workflows are. High quality anatomical models equipped with realistic fiber architecture, multiple label fields and pre-computed anatomical reference frames are becoming publicly available. A point in case is the recent study by Strocchi et al. [35] that placed in a repository a cohort of 24 volumetric four-chamber meshes derived from heart failure patients, which can be used for organ level simulations with *openCARP*. For cohort studies in healthy individuals, statistical shape models allow covering even more anatomical variability. Biventricular and biatrial shape models, together with 100 volumetric instances

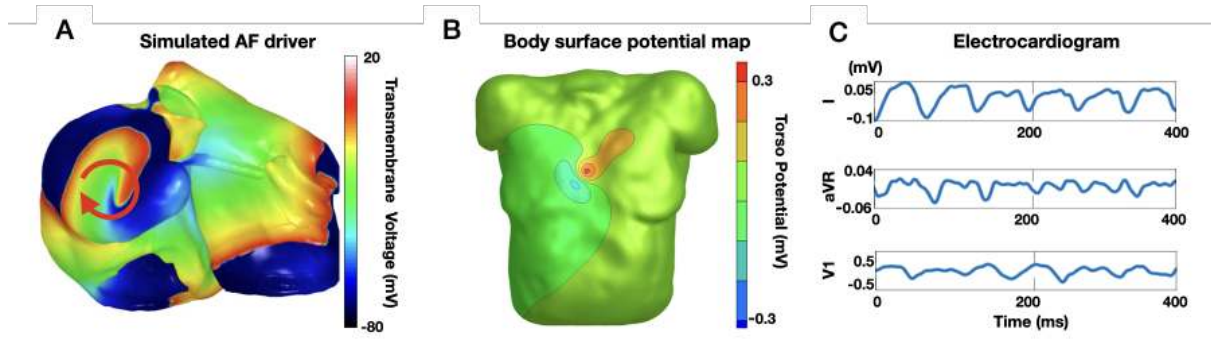


Figure 6: A: Biatrial volumetric model with ongoing reentry induced by pacing at the end of the refractory period using the *carputils* function `model.induceReentry.PEERP()`. B: Forward-calculated body surface potentials stemming from the transmembrane distribution in panel A. C: ECG (Einthoven lead I, Goldberger lead aVR and Wilson lead V1) extracted from the body surface potential map time series (panel B) reflecting the atrial fibrillation perpetuating at the tissue level (panel A).

418 ready to be used for *openCARP* simulation, are publicly available [110, 111]. It is anticipated and foreseeable
 419 that the number of publicly available anatomical twin models will further increase, hopefully in part due to the
 420 standardization of formats under *openCARP*, yielding an abundant pool of cardiac anatomy models available to
 421 *in silico* CEP research. For creating digital twin models based on data acquired from individual patients model
 422 parameters need to be identified that minimize the misfit between simulated and observed quantities [112]. Owing
 423 to their mechanistic nature, such digital twin models show promise as an approach towards realizing precision
 424 medicine where therapeutic responses simulated *in silico* may be used to guide therapy planning and delivery.
 425 For this purpose, largely automated pipelines have been proposed for the atria [72, 113], the ventricles and the
 426 whole heart [35, 53]. The geometric models can be augmented with population-level *a priori* knowledge regarding
 427 myocyte orientation in the atria [114, 115], the ventricles [107] or the whole heart [116]. Like anatomy, functional
 428 properties can be represented by population averages [117] or personalized using non-invasive or intracardiac
 429 measurements [72, 79, 118–121]. Depending on the scientific question, relevant parameters can be global or
 430 spatial distributions, and can include, for example, tissue conductivity, ionic model properties, or the initially
 431 activated sites. Generic frames of reference, such as the universal ventricular coordinates [95] or universal atrial
 432 coordinates [122] allow parametrizing locations within the cardiac chambers to facilitate optimization approaches
 433 and transferability between models.

434 A common use case for organ level simulations is assessing the effects on arrhythmia inducibility of factors
 435 like fibrosis, scar or drugs. *carputils* provides several arrhythmia induction methods [123] to efficiently build such
 436 *in silico* experiments. The basic use is illustrated in one of the currently 28 *carputils* examples in addition to the
 437 API documentation. Users can readily integrate these induction methods in their own *carputils* experiments.

438 `model.induceReentry.PEERP(..., stim_points, ...)`

439 calls the *carputils* function *PEERP* to apply a protocol which paces at the end of ERP (PEERP) from all points
 440 included in the `stim_points` list. Depending on the cellular and tissue properties, reentry can be induced as shown
 441 in Fig. 6A where a rotor at the left atrial appendage drives reentry in both atria. *Meshalyzer*, part of the *openCARP*
 442 ecosystem, was used to produce Fig. 6A. Alternatively, *openCARP* results can be directly output in VTK format,
 443 or converted to VTK format in a post-processing step, for seamless visualization in *ParaView* [94].

424 2.1.4 Body Level

425 Cardiac excitation and the resulting spatially heterogeneous transmembrane voltage distribution, $V_m(x, t)$, in cardiac
 426 tissue act as sources that generate electric current flow in the extracellular domain comprising the interstitial space
 427 as well as a volume conductor potentially surrounding the cardiac tissue (blood pool, torso), often referred to as
 428 bath. Currents in the volume conductor set up an extracellular potential field, $\Phi_e(x, t)$, that can be sampled by
 429 electrodes to acquire body surface potentials or intracardiac electrograms. Apart from experimental settings where
 430 cardiac sources in the form of $V_m(x, t)$ can be observed more directly [124, 125], extracellular potential recordings
 431 are the only means in the clinic to infer the cardiac source distribution. Owing to the unique importance of these

432 signals for diagnosis and guiding therapy, methodologies facilitating their accurate simulation are an indispensable
433 adjunct in many CEP simulation studies. These demands are reflected in the underlying bidomain equations solved
434 by *openCARP*, which comprise both computational domains, the intracellular domain and the extracellular domain,
435 thus facilitating the simulation of electrograms [75, 76, 126] or torso potentials [78, 120]. The electrical potential
436 within the volume of interest can be computed in *openCARP* using different methods depending on the trade-off
437 between computation and accuracy desired: i) The bidomain setting, which considers bath-loading effects [127]
438 and allows for bidirectional interplay between intracellular and extracellular potential fields; ii) Alternatively,
439 extracellular potential can be recovered in a post-processing step from a given spatiotemporal transmembrane
440 voltage distribution obtained through, a monodomain simulation. Bishop & Plank [128] showed that the latter
441 approach (referred to as *pseudo bidomain*) retains accuracy in most cases, particularly with augmentation techniques
442 to recover bath-loading effects close to the tissue-bath interface [129], while drastically reducing the computational
443 cost; and iii) An even more simplistic approach is to assume that the cardiac tissue is immersed in a homogeneous
444 volume conductor of infinite size, which allows recovering the extracellular potential Φ_e at specific points in space
445 from a given transmembrane voltage distribution by using the integral solution of Poisson's equation. One of
446 the *carputils examples* introduces all three methods and involves the user in simple experiments highlighting the
447 differences between them. To compute surface potentials in own *carputils* experiments, the `ep` module provides
448 the `model_type_opts(sourceModel)` function to choose between Φ_e recovery, pseudo-bidomain and bidomain.
449 Fig. 6B shows a snapshot of the body surface potential map generated by the transmembrane voltage distribution
450 V_m during atrial fibrillation shown in Fig. 6A. By extracting the time series of extracellular potentials $\Phi_e(t)$ at the
451 electrode locations, virtual ECGs can be derived by subtraction of electrograms along the lead axes (Fig. 6C).

452 3 Discussion

453 *openCARP* is a CEP simulation environment for carrying out advanced *in silico* experiments. The *openCARP*
454 framework is highly versatile and comprehensive, in principle allowing replicating and building on the vast majority
455 of published CEP simulation studies which rely only on the monodomain, bidomain and Poisson equations.
456 *openCARP* builds on the core technologies of its proprietary predecessors, *CARP* and *acCELLerate*, that have
457 matured over 20+ years of cutting edge modeling research, having been used in more than 250 published studies.
458 *openCARP* provides a convenient and flexible user interface that enables performing complex simulations, requiring
459 little to no programming experience. It supports the full research life cycle from exploration through to conclusive
460 analysis and publication, to archiving and sharing of data, experimental protocols, models and source code. As
461 such, *openCARP* can be a suitable software solution for a large portion of the CEP community, by contributing to
462 the use, transparency, standardization and reproducibility of *in silico* approaches.

463 *openCARP* is designed to appeal to users of all experience levels. New users can easily explore parameter
464 effects in prebuilt *carputils* experiments, while more experienced users can further extend such experiments to
465 more elaborate scenarios, or build their own complex experiments from scratch. *openCARP* provides a solution
466 for potential new users in the fields of basic science CEP (integrating experimental data into mechanistic models),
467 cardiology research (understanding arrhythmia mechanisms, diagnostic support, therapy stratification, planning
468 and delivery), pharmaceutical companies (virtual testing arrhythmogenic potency of new compounds), medical
469 device companies (interpreting measured signals, optimizing new device designs [130], testing their safety and
470 efficacy, and understanding reasons for device failure [26]), educational use (visualizing complex heart function),
471 and regulatory entities (e.g., the FDA which is already encouraging the use of numerical models for drug and device
472 testing [2]).

473 The central resource and entry point is the project web page www.openCARP.org. From there, the community
474 has access to the user and developer documentation, tutorials, *examples*, the GitLab projects, and a question and
475 answer system [131]. Besides the online platform, in-person contact among and between users and developers is
476 recognized as a key factor to build and maintain a strong community. Regular user meetings allow training new
477 users, exchange experiences with the software, and stay close with the community as part of a continuous feedback
478 loop. Within a year from the release of the first public version, more than 250 users opened an account in our user
479 and development community.

480 *openCARP* is a meritocratic, consensus-based community project. Anyone with an interest in the project can
481 join the community, contribute to the project design, and participate in the decision making process. Community
482 contributions are highly appreciated and can range from code commits to bug reports, suggestion of ideas and new
483 directions for improving the software, documentation or any aspect of the community platform. Code contributions
484 will enter a review process as a quality control measure and will be integrated in the code base if they meet quality
485 criteria and satisfy a community need. The roles in the *openCARP* project are *users*, *developers*, *maintainers* and
486 the *steering committee*. Users are community members who have a need for the project. The *openCARP* project
487 asks its users to participate in the project and community as much as possible. Contributors engage with the project

488 in concrete ways, through the issue tracker, question and answer system, or by writing or editing documentation.
489 They submit changes to the project itself via commits to non-protected branches of our git repositories, which then
490 undergo review by the maintainers before be merged into the main branch of code. Most of the 12 maintainers
491 and five steering committee members are employed on tenured stable academic positions, ensuring long-term
492 maintenance and support.

493 An important prerequisite for the reproducibility and reusability of models and associated simulation data is
494 their enrichment with metadata, and publication as FAIR [132] and open data. While *openCARP* carries the features
495 to reproduce the majority of published CEP simulations, the practical limitation is a not fully complete description
496 of experiments or limited data availability. We are, therefore, currently embedding mechanisms in *carputils*
497 to automate the extraction of all relevant information for a specific experiment, and create packages suitable for
498 archiving and sharing. A convenient interface to upload these simulation packages to an *openCARP* specific section
499 of the [RADAR4KIT research data repository](#) [133] will be provided in the near future. RADAR4KIT is a long-term
500 research data repository that adheres to the Open Archival Information System (OAIS) standard [134]. It provides
501 access control (public, private sharing via link), persistent DOI identifiers, standardized interfaces facilitating data
502 harvesting, and is integrated with research data meta repositories like re3data [135]. In this way, the *carputils*
503 experiment can be further evaluated by the scientific community, and future research can build upon it. Errors or
504 previously undiscovered artifacts can be found and described, leading to improved data and research quality in the
505 long term as one of the main goals of open science.

506 In conclusion, *openCARP* is an open CEP simulator released to the academic community to advance the
507 computational CEP field by making state-of-the-art simulations accessible. A commercial license can be requested.
508 In combination with the open source *carputils* framework and additional open source software around it, it offers
509 a tailored software solution for the scientific community in the CEP field and contributes towards increasing use,
510 transparency, standardization and reproducibility of *in silico* experiments.

511 Acknowledgments

512 We gratefully acknowledge support by Deutsche Forschungsgemeinschaft (DFG) (project ID 391128822, LO
513 2093/1-1, GS 1758/4-1). We further acknowledge the software contributions of NumeriCor GmbH, Graz, Austria
514 who conceived and implemented the *openCARP* simulation core. We thank Felix Bach, Jochen Klar and Robert
515 Ulrich for developing and providing the *openCARP development environment* as well as Michael Selzer and Philipp
516 Zschumme for developing and providing *toolcompendium* for generation of user documentation. We thank Prof.
517 Natalia Trayanova for agreeing to make the *EasyML* model generator, developed in her lab by Rob Blake, available
518 to be distributed with *openCARP*. We thank Giorgio Luongo for providing figures of simulation results.

519 Conflicts of interest

520 GP, AN, CA and EJV are co-founders of NumeriCor GmbH. All other authors declare no conflict of interest.

521 References

- 522 [1] S. A. Niederer, J. Lumens, and N. A. Trayanova, “Computational models in cardiology.” *Nature Reviews.*
523 *Cardiology*, 10 2018. doi:[10.1038/s41569-018-0104-y](https://doi.org/10.1038/s41569-018-0104-y)
- 524 [2] US Food and Drug Administration, “Reporting of computational modeling studies in medical device sub-
525 missions,” 2016.
- 526 [3] J. Corral-Acero, F. Margara, M. Marciniak *et al.*, “The ‘digital twin’ to enable the vision of precision
527 cardiology.” *European heart journal*, 3 2020. doi:[10.1093/eurheartj/ehaa159](https://doi.org/10.1093/eurheartj/ehaa159)
- 528 [4] D. G. Whittaker, R. A. Capel, M. Hendrix, X. H. S. Chan, N. Herring, N. J. White, G. R.
529 Mirams, and R.-A. B. Burton, “Cardiac TdP risk stratification modelling of anti-infective compounds
530 including chloroquine and hydroxychloroquine,” *Royal Society Open Science*, vol. 8, no. 4, Apr. 2021.
531 doi:[10.1098/rsos.210235](https://doi.org/10.1098/rsos.210235). <https://doi.org/10.1098/rsos.210235>
- 532 [5] S. Gaeta, T. D. Bahnson, and C. Henriquez, “Mechanism and magnitude of bipolar electrogram directional
533 sensitivity: Characterizing underlying determinants of bipolar amplitude,” *Heart Rhythm*, vol. 17, no. 5,
534 pp. 777–785, May 2020. doi:[10.1016/j.hrthm.2019.12.010](https://doi.org/10.1016/j.hrthm.2019.12.010). <https://doi.org/10.1016/j.hrthm.2019.12.010>

- 535 [6] F. Margara, Z. J. Wang, F. Levrero-Florencio, A. Santiago, M. Vázquez, A. Bueno-Orovio, and B. Rodriguez,
536 “In-silico human electro-mechanical ventricular modelling and simulation for drug-induced pro-arrhythmia
537 and inotropic risk assessment,” *Progress in Biophysics and Molecular Biology*, vol. 159, pp. 58–74, Jan.
538 2021. doi:[10.1016/j.pbiomolbio.2020.06.007](https://doi.org/10.1016/j.pbiomolbio.2020.06.007). <https://doi.org/10.1016/j.pbiomolbio.2020.06.007>
- 539 [7] M. Paci, J. T. Koivumäki, H. R. Lu, D. J. Gallacher, E. Passini, and B. Rodriguez, “Comparison of the
540 simulated response of three in silico human stem cell-derived cardiomyocytes models and in vitro data
541 under 15 drug actions,” *Frontiers in Pharmacology*, vol. 12, Mar. 2021. doi:[10.3389/fphar.2021.604713](https://doi.org/10.3389/fphar.2021.604713).
542 <https://doi.org/10.3389/fphar.2021.604713>
- 543 [8] A. Gharaviri, S. Pezzuto, M. Potse, S. Verheule, G. Conte, R. Krause, U. Schotten, and
544 A. Auricchio, “Left atrial appendage electrical isolation reduces atrial fibrillation recurrences,”
545 *Circulation: Arrhythmia and Electrophysiology*, vol. 14, no. 1, Jan. 2021. doi:[10.1161/circep.120.009230](https://doi.org/10.1161/circep.120.009230).
546 <https://doi.org/10.1161/circep.120.009230>
- 547 [9] S. A. Niederer, E. Kerfoot, A. P. Benson *et al.*, “Verification of cardiac tissue electrophysiology simulators
548 using an n-version benchmark,” *Philosophical Transactions of the Royal Society A: Mathematical, Physical*
549 *and Engineering Sciences*, vol. 369, no. 1954, pp. 4331–4351, 2011. doi:[10.1098/rsta.2011.0139](https://doi.org/10.1098/rsta.2011.0139)
- 550 [10] R. C. Barr and R. Plonsey, “Propagation of excitation in idealized anisotropic two-dimensional tissue.”
551 *Biophys. J.*, vol. 45, no. 6, pp. 1191–202, jun 1984. doi:[10.1016/S0006-3495\(84\)84268-X](https://doi.org/10.1016/S0006-3495(84)84268-X)
- 552 [11] M. S. Spach and J. M. Kootsey, “Relating the sodium current and conductance to the shape of transmembrane
553 and extracellular potentials by simulation: effects of propagation boundaries.” *IEEE Trans. Biomed. Eng.*,
554 vol. 32, no. 10, pp. 743–55, oct 1985. doi:[10.1109/TBME.1985.325489](https://doi.org/10.1109/TBME.1985.325489)
- 555 [12] B. Baillargeon, N. Rebelo, D. D. Fox, R. L. Taylor, and E. Kuhl, “The Living Heart Project: A ro-
556 bust and integrative simulator for human heart function,” *Eur. J. Mech. - A/Solids*, pp. 1–10, apr 2014.
557 doi:[10.1016/j.euromechsol.2014.04.001](https://doi.org/10.1016/j.euromechsol.2014.04.001)
- 558 [13] M. J. Bishop and G. Plank, “The role of fine-scale anatomical structure in the dynamics of reentry in
559 computational models of the rabbit ventricles.” *J Physiol*, vol. 590, no. Pt 18, pp. 4515–4535, sep 2012.
560 doi:[10.1113/jphysiol.2012.229062](https://doi.org/10.1113/jphysiol.2012.229062)
- 561 [14] M. Strocchi, A. W. Lee, A. Neic *et al.*, “His Bundle and Left Bundle Pacing with Optimised Atrio-ventricular
562 Delay Achieve Superior Electrical Synchrony over Endocardial and Epicardial Pacing in Left Bundle Branch
563 Block Patients,” *Heart Rhythm*, 2020. doi:[10.1016/j.hrthm.2020.06.028](https://doi.org/10.1016/j.hrthm.2020.06.028)
- 564 [15] E. J. Vigmond and L. J. Leon, “Computationally efficient model for simulating electrical activity in cardiac
565 tissue with fiber rotation.” *Ann. Biomed. Eng.*, vol. 27, no. 2, pp. 160–70, 1999. doi:[10.1114/1.160](https://doi.org/10.1114/1.160)
- 566 [16] E. J. Vigmond, M. Hughes, G. Plank, and L. J. Leon, “Computational tools for modeling electrical activity
567 in cardiac tissue,” *J Electrocardiol*, vol. 36 Suppl, pp. 69–74, 2003. doi:[10.1016/j.jelectrocard.2003.09.017](https://doi.org/10.1016/j.jelectrocard.2003.09.017)
- 568 [17] G. Seemann, F. B. Sachse, M. Karl, D. L. Weiss, V. Heuveline, and O. Dössel, “Framework for modular,
569 flexible and efficient solving the cardiac bidomain equation using PETSc,” *Mathematics in Industry*, vol. 15,
570 no. 2, pp. 363–369, 1 2010. doi:[10.1007/978-3-642-12110-4_55](https://doi.org/10.1007/978-3-642-12110-4_55)
- 571 [18] C. Bradley, A. Bowery, R. Britten *et al.*, “OpenCMISS: a multi-physics & multi-scale computational
572 infrastructure for the VPH/physiome project.” *Progress in biophysics and molecular biology*, vol. 107, no. 1,
573 pp. 32–47, 10 2011. doi:[10.1016/j.pbiomolbio.2011.06.015](https://doi.org/10.1016/j.pbiomolbio.2011.06.015)
- 574 [19] M.-C. Trudel, B. Dubé, M. Potse, R. M. Gulrajani, and L. J. Leon, “Simulation of QRST integral maps with
575 a membrane-based computer heart model employing parallel processing.” *IEEE transactions on bio-medical*
576 *engineering*, vol. 51, no. 8, pp. 1319–29, 8 2004. doi:[10.1109/TBME.2004.827934](https://doi.org/10.1109/TBME.2004.827934)
- 577 [20] M. B. Liu, E. de Lange, A. Garfinkel, J. N. Weiss, and Z. Qu, “Delayed afterdepolarizations generate both
578 triggers and a vulnerable substrate promoting reentry in cardiac tissue.” *Heart rhythm*, vol. 12, no. 10, pp.
579 2115–24, 10 2015. doi:[10.1016/j.hrthm.2015.06.019](https://doi.org/10.1016/j.hrthm.2015.06.019)
- 580 [21] E. A. Heidenreich, J. M. Ferrero, M. Doblaré, and J. F. Rodríguez, “Adaptive macro finite elements for the
581 numerical solution of monodomain equations in cardiac electrophysiology,” *Ann. Biomed. Eng.*, vol. 38,
582 no. 7, pp. 2331–2345, 2010. doi:[10.1007/s10439-010-9997-2](https://doi.org/10.1007/s10439-010-9997-2)
- 583 [22] K. P. Vincent, M. J. Gonzales, A. K. Gillette, C. T. Villongco, S. Pezzuto, J. H. Omens, M. J. Holst, and
584 A. D. McCulloch, “High-order finite element methods for cardiac monodomain simulations.” *Front. Physiol.*,
585 vol. 6, no. August, p. 217, 2015. doi:[10.3389/fphys.2015.00217](https://doi.org/10.3389/fphys.2015.00217)

- 586 [23] F. H. Fenton, E. M. Cherry, H. M. Hastings, and S. J. Evans, "Multiple mechanisms of spiral wave breakup
587 in a model of cardiac electrical activity," *Chaos (Woodbury, N.Y.)*, vol. 12, no. 3, pp. 852–892, 1 2002.
588 doi:[10.1063/1.1504242](https://doi.org/10.1063/1.1504242)
- 589 [24] M. J. Bishop, E. J. Vigmond, and G. Plank, "The functional role of electrophysiological heterogeneity in the
590 rabbit ventricle during rapid pacing and arrhythmias." *Am. J. Physiol. Heart Circ. Physiol.*, vol. 304, no. 9,
591 pp. H1240–52, 2013. doi:[10.1152/ajpheart.00894.2012](https://doi.org/10.1152/ajpheart.00894.2012)
- 592 [25] A. Loewe, E. Poremba, T. Oesterlein, A. Luik, C. Schmitt, G. Seemann, and O. Dössel, "Patient-specific
593 identification of atrial flutter vulnerability—a computational approach to reveal latent reentry pathways,"
594 *Frontiers in Physiology*, vol. 9, no. Article 1910, 1 2019. doi:[10.3389/fphys.2018.01910](https://doi.org/10.3389/fphys.2018.01910)
- 595 [26] D. J. Swenson, R. T. Taepke, J. J. Blauer, E. Kwan, E. Ghafoori, G. Plank, E. Vigmond, R. S. MacLeod,
596 P. DeGroot, and R. Ranjan, "Direct comparison of a novel antitachycardia pacing algorithm against
597 present methods using virtual patient modeling," *Hear. Rhythm*, vol. 17, no. 9, pp. 1602–1608, 2020.
598 doi:[10.1016/j.hrthm.2020.05.009](https://doi.org/10.1016/j.hrthm.2020.05.009)
- 599 [27] G. Plank, L. J. Leon, S. Kimber, and E. J. Vigmond, "Defibrillation depends on conductivity fluctuations
600 and the degree of disorganization in reentry patterns." *J. Cardiovasc. Electrophysiol.*, vol. 16, no. 2, pp.
601 205–16, feb 2005. doi:[10.1046/j.1540-8167.2005.40140.x](https://doi.org/10.1046/j.1540-8167.2005.40140.x)
- 602 [28] A. Loewe, Y. Lutz, M. Wilhelms, D. Sinnecker, P. Barthel, E. P. Scholz, O. Dössel, G. Schmidt, and
603 G. Seemann, "In-silico assessment of the dynamic effects of amiodarone and dronedarone on human atrial
604 patho-electrophysiology." *Europace*, vol. 16, no. S4, pp. iv30–iv38, 11 2014. doi:[10.1093/europace/euu230](https://doi.org/10.1093/europace/euu230)
- 605 [29] H. Anzt, F. Bach, S. Druskat *et al.*, "An environment for sustainable research software in germany and
606 beyond: current state, open challenges, and call for action," *F1000Research*, vol. 9, p. 295, 1 2020.
607 doi:[10.12688/f1000research.23224.1](https://doi.org/10.12688/f1000research.23224.1)
- 608 [30] G. W. Beeler and H. Reuter, "Reconstruction of the action potential of ventricular myocardial fibers," *Journal*
609 *of Physiology*, vol. 268, pp. 177–210, 1 1977. doi:[10.1113/jphysiol.1977.sp011853](https://doi.org/10.1113/jphysiol.1977.sp011853)
- 610 [31] L. Ebihara and E. A. Johnson, "Fast sodium current in cardiac muscle. a quantitative description," *Biophysical*
611 *Journal*, vol. 32, pp. 779–790, 1 1980. doi:[10.1016/S0006-3495\(80\)85016-8](https://doi.org/10.1016/S0006-3495(80)85016-8)
- 612 [32] C. H. Luo and Y. Rudy, "A model of the ventricular cardiac action potential. depolarization, repolarization,
613 and their interaction," *Circulation Research*, vol. 68, pp. 1501–1526, 1 1991. doi:[10.1161/01.RES.68.6.1501](https://doi.org/10.1161/01.RES.68.6.1501)
- 614 [33] E. J. Vigmond, F. Aguel, and N. a. Trayanova, "Computational techniques for solving the bidomain
615 equations in three dimensions." *IEEE Trans. Biomed. Eng.*, vol. 49, no. 11, pp. 1260–9, nov 2002.
616 doi:[10.1109/TBME.2002.804597](https://doi.org/10.1109/TBME.2002.804597)
- 617 [34] D. M. Harrild and C. S. Henriquez, "A computer model of the normal conduction in the human atria," *Circ.*
618 *Res.*, 2004. doi:[10.1161/01.RES.0000148636.60732.2e](https://doi.org/10.1161/01.RES.0000148636.60732.2e)
- 619 [35] M. Strocchi, C. M. Augustin, M. A. F. Gsell *et al.*, "A publicly available virtual cohort of four-chamber
620 heart meshes for cardiac electro-mechanics simulations." *PloS one*, vol. 15, no. 6, p. e0235145, 1 2020.
621 doi:[10.1371/journal.pone.0235145](https://doi.org/10.1371/journal.pone.0235145)
- 622 [36] S. R. Kharche, E. Vigmond, I. R. Efimov, and H. Dobrzynski, "Computational assessment of the functional
623 role of sinoatrial node exit pathways in the human heart." *PloS one*, vol. 12, no. 9, p. e0183727, 1 2017.
624 doi:[10.1371/journal.pone.0183727](https://doi.org/10.1371/journal.pone.0183727)
- 625 [37] A. Loewe, Y. Lutz, N. Nagy, A. Fabbri, C. Schweda, A. Varro, and S. Severi, "Inter-species differences
626 in the response of sinus node cellular pacemaking to changes of extracellular calcium," in *41st Annual*
627 *International Conference of the IEEE Engineering in Medicine and Biology Society (EMBC)*, 2019, pp.
628 1875–1878. doi:[10.1109/EMBC.2019.8857573](https://doi.org/10.1109/EMBC.2019.8857573)
- 629 [38] A. Loewe, Y. Lutz, D. Nairn *et al.*, "Hypocalcemia-induced slowing of human sinus node pacemaking,"
630 *Biophysical Journal*, vol. 117, no. 12, pp. 2244–2254, 1 2019. doi:[10.1016/j.bpj.2019.07.037](https://doi.org/10.1016/j.bpj.2019.07.037)
- 631 [39] J. Li, I. D. Greener, S. Inada *et al.*, "Computer three-dimensional reconstruction of the atrioventricular node." *Circulation research*, vol. 102, no. 8, pp. 975–85, 4 2008. doi:[10.1161/CIRCRESAHA.108.172403](https://doi.org/10.1161/CIRCRESAHA.108.172403)
- 632
633 [40] E. J. Vigmond and B. D. Stuyvers, "Modeling our understanding of the his-purkinje system." *Progress in bio-*
634 *physics and molecular biology*, vol. 120, no. 1-3, pp. 179–88, 1 2016. doi:[10.1016/j.pbiomolbio.2015.12.013](https://doi.org/10.1016/j.pbiomolbio.2015.12.013)

- 635 [41] A. Loewe, E. M. Wülfers, and G. Seemann, “Cardiac ischemia-insights from computational models.”
636 *Herzschrittmachertherapie & Elektrophysiologie*, vol. 29, no. 1, pp. 48–56, 3 2018. doi:[10.1007/s00399-](https://doi.org/10.1007/s00399-017-0539-6)
637 [017-0539-6](https://doi.org/10.1007/s00399-017-0539-6)
- 638 [42] C. M. Costa, A. Neic, E. Kerfoot *et al.*, “Pacing in proximity to scar during cardiac resynchronization
639 therapy increases local dispersion of repolarization and susceptibility to ventricular arrhythmogenesis.”
640 *Heart rhythm*, 3 2019. doi:[10.1016/j.hrthm.2019.03.027](https://doi.org/10.1016/j.hrthm.2019.03.027)
- 641 [43] C. H. Roney, J. D. Bayer, S. Zahid, M. Meo, P. M. J. Boyle, N. A. Trayanova, M. Haïssaguerre, R. Dubois,
642 H. Cochet, and E. J. Vigmond, “Modelling methodology of atrial fibrosis affects rotor dynamics and
643 electrograms.” *Europace*, vol. 18, no. suppl 4, pp. iv146–iv155, 12 2016. doi:[10.1093/europace/euw365](https://doi.org/10.1093/europace/euw365)
- 644 [44] A. Jadidi, M. Nothstein, J. Chen *et al.*, “Specific electrogram characteristics identify the extra-pulmonary vein
645 arrhythmogenic sources of persistent atrial fibrillation - characterization of the arrhythmogenic electrogram
646 patterns during atrial fibrillation and sinus rhythm.” *Scientific Reports*, vol. 10, no. 1, p. 9147, 6 2020.
647 doi:[10.1038/s41598-020-65564-2](https://doi.org/10.1038/s41598-020-65564-2)
- 648 [45] G. Balaban, B. P. Halliday, C. Mendonca Costa, W. Bai, B. Porter, C. A. Rinaldi, G. Plank, D. Rueckert,
649 S. K. Prasad, and M. J. Bishop, “Fibrosis microstructure modulates reentry in non-ischemic dilated car-
650 diomyopathy: Insights from imaged guided 2d computational modeling,” *Frontiers in Physiology*, vol. 9, 1
651 2018. doi:[10.3389/fphys.2018.01832](https://doi.org/10.3389/fphys.2018.01832)
- 652 [46] L. Zhou, S. Solhjoo, B. Millare, G. Plank, M. R. Abraham, S. Cortassa, N. Trayanova, and B. O’Rourke, “Ef-
653 fects of regional mitochondrial depolarization on electrical propagation: implications for arrhythmogenesis.”
654 *Circ. Arrhythm. Electrophysiol.*, vol. 7, no. 1, pp. 143–51, 2014. doi:[10.1161/CIRCEP.113.000600](https://doi.org/10.1161/CIRCEP.113.000600)
- 655 [47] G. Plank, R. A. B. Burton, P. Hales *et al.*, “Generation of histo-anatomically representative models of
656 the individual heart: tools and application,” *Philos Trans A Math Phys Eng Sci*, vol. 367, no. 1896, pp.
657 2257–2292, 2009. doi:[10.1098/rsta.2009.0056](https://doi.org/10.1098/rsta.2009.0056)
- 658 [48] M. J. Bishop, G. Plank, R. A. B. Burton, J. E. Schneider, D. J. Gavaghan, V. Grau, and P. Kohl, “Development
659 of an anatomically detailed MRI-derived rabbit ventricular model and assessment of its impact on simulations
660 of electrophysiological function.” *American Journal of Physiology. Heart and Circulatory Physiology*, vol.
661 298, no. 2, pp. H699–718, 2 2010. doi:[10.1152/ajpheart.00606.2009](https://doi.org/10.1152/ajpheart.00606.2009)
- 662 [49] G. Seemann, A. Loewe, and E. M. Wülfers, “Effects of fibroblasts coupling on the electrophysiology
663 of cardiomyocytes from different regions of the human atrium: A simulation study,” in *Computing in*
664 *Cardiology*, vol. 44, 2017. doi:[10.22489/CinC.2017.380-451](https://doi.org/10.22489/CinC.2017.380-451)
- 665 [50] C. M. Costa, F. O. Campos, A. J. Prassl, R. W. dos Santos, D. Sanchez-Quintana, H. Ahammer, E. Hofer, and
666 G. Plank, “An efficient finite element approach for modeling fibrotic clefts in the heart,” *IEEE Transactions*
667 *on Biomedical Engineering*, vol. 61, no. 3, pp. 900–910, 1 2014. doi:[10.1109/TBME.2013.2292320](https://doi.org/10.1109/TBME.2013.2292320)
- 668 [51] T. Yu, C. M. Lloyd, D. P. Nickerson *et al.*, “The Physiome Model Repository 2,” *Bioinformatics*, vol. 27,
669 no. 5, pp. 743–744, 01 2011. doi:[10.1093/bioinformatics/btq723](https://doi.org/10.1093/bioinformatics/btq723)
- 670 [52] A. J. Prassl, F. Kicking, H. Ahammer, V. Grau, J. E. Schneider, E. Hofer, E. J. Vigmond, N. a. Trayanova, and
671 G. Plank, “Automatically generated, anatomically accurate meshes for cardiac electrophysiology problems,”
672 *IEEE Trans. Biomed. Eng.*, vol. 56, no. 5, pp. 1318–1330, may 2009. doi:[10.1109/TBME.2009.2014243](https://doi.org/10.1109/TBME.2009.2014243)
- 673 [53] A. Crozier, C. M. Augustin, A. Neic *et al.*, “Image-based personalization of cardiac anatomy for coupled
674 electromechanical modeling,” *Annals of Biomedical Engineering*, 1 2015. doi:[10.1007/s10439-015-1474-5](https://doi.org/10.1007/s10439-015-1474-5)
- 675 [54] A. Neic, M. A. Gsell, E. Karabelas, A. J. Prassl, and G. Plank, “Automating image-based mesh generation
676 and manipulation tasks in cardiac modeling workflows using meshtool,” *SoftwareX*, vol. 11, p. 100454, 1
677 2020. doi:[10.1016/j.softx.2020.100454](https://doi.org/10.1016/j.softx.2020.100454)
- 678 [55] M. L. Hines and N. T. Carnevale, “NEURON: a tool for neuroscientists.” *The Neuroscientist : a re-*
679 *view journal bringing neurobiology, neurology and psychiatry*, vol. 7, no. 2, pp. 123–35, 4 2001.
680 doi:[10.1177/107385840100700207](https://doi.org/10.1177/107385840100700207)
- 681 [56] G. M. J. Barca, C. Bertoni, L. Carrington *et al.*, “Recent developments in the general atomic and molecular
682 electronic structure system,” *The Journal of Chemical Physics*, vol. 152, no. 15, p. 154102, Apr. 2020.
683 doi:[10.1063/5.0005188](https://doi.org/10.1063/5.0005188)

- 684 [57] G. R. Mirams, C. J. Arthurs, M. O. Bernabeu *et al.*, “Chaste: an open source c++ library for computational physiology and biology,” *PLoS Computational Biology*, vol. 9, no. 3, p. e1002970, 1 2013.
685 doi:[10.1371/journal.pcbi.1002970](https://doi.org/10.1371/journal.pcbi.1002970)
686
- 687 [58] S. Pezzuto, F. W. Prinzen, M. Potse, F. Maffessanti, F. Regoli, M. L. Caputo, G. Conte, R. Krause, and
688 A. Auricchio, “Reconstruction of three-dimensional biventricular activation based on the 12-lead electro-
689 cardiogram via patient-specific modelling,” *EP Europace*, 1 2020. doi:[10.1093/europace/euaa330](https://doi.org/10.1093/europace/euaa330)
- 690 [59] A. Quarteroni, T. Lassila, S. Rossi, and R. Ruiz-Baier, “Integrated heart—coupling multiscale and multi-
691 physics models for the simulation of the cardiac function,” *Computer Methods in Applied Mechanics and*
692 *Engineering*, vol. 314, pp. 345–407, 1 2017. doi:[10.1016/j.cma.2016.05.031](https://doi.org/10.1016/j.cma.2016.05.031)
- 693 [60] P. Colli Franzone, L. F. Pavarino, and S. Scacchi, “A numerical study of scalable cardiac electro-mechanical
694 solvers on HPC architectures,” *Frontiers in Physiology*, vol. 9, 1 2018. doi:[10.3389/fphys.2018.00268](https://doi.org/10.3389/fphys.2018.00268)
- 695 [61] R. H. Clayton and A. V. Holden, “Propagation of normal beats and re-entry in a computational model of
696 ventricular cardiac tissue with regional differences in action potential shape and duration,” *Prog. Biophys.*
697 *Mol. Biol.*, vol. 85, no. 2-3, pp. 473–499, 1 2004. doi:[10.1016/j.pbiomolbio.2003.12.002](https://doi.org/10.1016/j.pbiomolbio.2003.12.002)
- 698 [62] J. Sundnes, S. Wall, H. Osnes, T. Thorvaldsen, and A. D. McCulloch, “Improved discretisation
699 and linearisation of active tension in strongly coupled cardiac electro-mechanics simulations,” *Com-*
700 *puter Methods in Biomechanics and Biomedical Engineering*, vol. 17, no. 6, pp. 604–615, 1 2014.
701 doi:[10.1080/10255842.2012.704368](https://doi.org/10.1080/10255842.2012.704368)
- 702 [63] M. Antonioletti, V. N. Biktashev, A. Jackson, S. R. Khariche, T. Stary, and I. V. Biktasheva, “Beatbox—hpc
703 simulation environment for biophysically and anatomically realistic cardiac electrophysiology,” *PLOS ONE*,
704 vol. 12, no. 5, pp. 1–37, 05 2017. doi:[10.1371/journal.pone.0172292](https://doi.org/10.1371/journal.pone.0172292)
- 705 [64] J. Koehler Leman, B. D. Weitzner, P. D. Renfrew *et al.*, “Better together: Elements of successful scientific
706 software development in a distributed collaborative community,” *PLOS Computational Biology*, vol. 16,
707 no. 5, pp. 1–20, 05 2020. doi:[10.1371/journal.pcbi.1007507](https://doi.org/10.1371/journal.pcbi.1007507). <https://doi.org/10.1371/journal.pcbi.1007507>
- 708 [65] B. Shneiderman, *Designing the User Interface: Strategies for Effective Human-Computer Interaction*, 3rd ed.
709 USA: Addison-Wesley Longman Publishing Co., Inc., 1997. ISBN 0201694972
- 710 [66] G. Wang and B. Peng, “Script of scripts: A pragmatic workflow system for daily computational research,”
711 *PLOS Computational Biology*, vol. 15, no. 2, pp. 1–14, 02 2019. doi:[10.1371/journal.pcbi.1006843](https://doi.org/10.1371/journal.pcbi.1006843).
712 <https://doi.org/10.1371/journal.pcbi.1006843>
- 713 [67] D. S. Katz, L. C. McInnes, D. E. Bernholdt *et al.*, “Community organizations: Changing the culture in which
714 research software is developed and sustained,” *Computing in Science & Engineering*, vol. 21, pp. 8–24, 3
715 2019. doi:[10.1109/MCSE.2018.2883051](https://doi.org/10.1109/MCSE.2018.2883051)
- 716 [68] S. Niederer, L. Mitchell, N. Smith, and G. Plank, “Simulating human cardiac electrophysiology
717 on clinical time-scales,” *Frontiers in Physiology*, vol. 2, p. 14, 2011. doi:[10.3389/fphys.2011.00014](https://doi.org/10.3389/fphys.2011.00014).
718 <https://www.frontiersin.org/article/10.3389/fphys.2011.00014>
- 719 [69] B. D. Lee, “Ten simple rules for documenting scientific software,” *PLOS Computational Biology*, vol. 14,
720 no. 12, pp. 1–6, 12 2018. doi:[10.1371/journal.pcbi.1006561](https://doi.org/10.1371/journal.pcbi.1006561). <https://doi.org/10.1371/journal.pcbi.1006561>
- 721 [70] W. J. Schroeder, K. Martin, and B. Lorensen, *The visualization toolkit*, 4th ed. Kitware, 2006.
- 722 [71] E. J. Vigmond, R. Weber dos Santos, A. J. Prassl, M. Deo, and G. Plank, “Solvers for the cardiac bidomain
723 equations,” *Progress in Biophysics and Molecular Biology*, vol. 96, no. 1-3, pp. 3–18, 1 2008.
724 doi:[10.1016/j.pbiomolbio.2007.07.012](https://doi.org/10.1016/j.pbiomolbio.2007.07.012)
- 725 [72] M. W. Krueger, G. Seemann, K. Rhode, D. U. J. Keller, C. Schilling, A. Arujuna, J. Gill, M. D. O’Neill,
726 R. Razavi, and O. Dössel, “Personalization of atrial anatomy and electrophysiology as a basis for clinical
727 modeling of radio-frequency ablation of atrial fibrillation,” *IEEE Transactions on Medical Imaging*, vol. 32,
728 no. 1, pp. 73–84, 1 2013. doi:[10.1109/TMI.2012.2201948](https://doi.org/10.1109/TMI.2012.2201948)
- 729 [73] F. O. Campos, Y. Shiferaw, A. J. Prassl, P. M. Boyle, E. J. Vigmond, and G. Plank, “Stochastic sponta-
730 neous calcium release events trigger premature ventricular complexes by overcoming electrotonic load.”
731 *Cardiovascular research*, vol. 107, no. 1, pp. 175–83, 7 2015. doi:[10.1093/cvr/cvv149](https://doi.org/10.1093/cvr/cvv149)
- 732 [74] A. Loewe, M. Wilhelms, F. Fischer, E. P. Scholz, O. Dössel, and G. Seemann, “Arrhythmic potency of
733 human ether-a-go-go-related gene mutations l532p and n588k in a computational model of human atrial
734 myocytes,” *Europace*, vol. 16, no. 3, pp. 435–443, 1 2014. doi:[10.1093/europace/eut375](https://doi.org/10.1093/europace/eut375)

- 735 [75] E. Vigmond, A. Pashaei, S. Amraoui, H. Cochet, and M. Hassaguerre, “Percolation as a mechanism to
736 explain atrial fractionated electrograms and reentry in a fibrosis model based on imaging data,” *Heart*
737 *Rhythm : the Official Journal of the Heart Rhythm Society*, vol. 13, no. 7, pp. 1536–1543, 1 2016.
738 doi:[10.1016/j.hrthm.2016.03.019](https://doi.org/10.1016/j.hrthm.2016.03.019)
- 739 [76] M. Alessandrini, M. Valinoti, L. Unger, T. Oesterlein, O. Dössel, C. Corsi, A. Loewe, and S. Severi, “A
740 computational framework to benchmark basket catheter guided ablation in atrial fibrillation,” *Frontiers in*
741 *Physiology*, vol. 9, p. 1251, 1 2018. doi:[10.3389/fphys.2018.01251](https://doi.org/10.3389/fphys.2018.01251)
- 742 [77] H. J. Arevalo, F. Vadakkumpadan, E. Guallar, A. Jebb, P. Malamas, K. C. Wu, and N. A. Trayanova,
743 “Arrhythmia risk stratification of patients after myocardial infarction using personalized heart models,”
744 *Nature Communications*, vol. 7, p. 11437, 1 2016. doi:[10.1038/ncomms11437](https://doi.org/10.1038/ncomms11437)
- 745 [78] R. Andlauer, G. Seemann, L. Baron, O. Dössel, P. Kohl, P. Platonov, and A. Loewe, “Influence of left atrial
746 size on p-wave morphology: differential effects of dilation and hypertrophy,” *Europace*, vol. 20, no. S3, pp.
747 iii36–iii44, 11 2018. doi:[10.1093/europace/euy231](https://doi.org/10.1093/europace/euy231)
- 748 [79] A. Prakosa, H. J. Arevalo, D. Deng *et al.*, “Personalized virtual-heart technology for guiding the ablation of
749 infarct-related ventricular tachycardia,” *Nature Biomedical Engineering*, 1 2018. doi:[10.1038/s41551-018-](https://doi.org/10.1038/s41551-018-0282-2)
750 [0282-2](https://doi.org/10.1038/s41551-018-0282-2)
- 751 [80] H. Lehrmann, A. S. Jadidi, J. Minners, J. Chen, B. Müller-Edenborn, R. Weber, O. Dössel, T. Arentz, and
752 A. Loewe, “Novel electrocardiographic criteria for real-time assessment of anterior mitral line block,” *JACC:*
753 *Clinical Electrophysiology*, vol. 4, no. 7, pp. 920–932, 1 2018. doi:[10.1016/j.jacep.2018.03.007](https://doi.org/10.1016/j.jacep.2018.03.007)
- 754 [81] B. M. Rocha, F. Kickingger, A. J. Prassl, G. Haase, E. J. Vigmond, R. W. Dos Santos, S. Zaglmayr,
755 and G. Plank, “A macro finite-element formulation for cardiac electrophysiology simulations using
756 hybrid unstructured grids,” *IEEE Trans. Biomed. Eng.*, vol. 58, no. 4, pp. 1055–1065, apr 2011.
757 doi:[10.1109/TBME.2010.2064167](https://doi.org/10.1109/TBME.2010.2064167). [http://ieeexplore.ieee.org/xpls/abs{
758 \[82\] C. M. Augustin, A. Neic, M. Liebmann, A. J. Prassl, S. A. Niederer, G. Haase, and G. Plank,
759 “Anatomically accurate high resolution modeling of human whole heart electromechanics: A strongly
760 scalable algebraic multigrid solver method for nonlinear deformation.” *J. Comput. Phys.*, vol. 305, pp.
761 622–646, jan 2016. doi:\[10.1016/j.jcp.2015.10.045\]\(https://doi.org/10.1016/j.jcp.2015.10.045\). <http://www.ncbi.nlm.nih.gov/pubmed/26819483><http://www.ncbi.nlm.nih.gov/pubmed/26819483>
762 <http://www.ncbi.nlm.nih.gov/pubmed/26819483>
763 \[83\] J. A. Southern, G. Plank, E. J. Vigmond, and J. P. Whiteley, “Solving the coupled system improves
764 computational efficiency of the bidomain equations.” *IEEE Trans. Biomed. Eng.*, vol. 56, no. 10, pp.
765 2404–12, oct 2009. doi:\[10.1109/TBME.2009.2022548\]\(https://doi.org/10.1109/TBME.2009.2022548\). <http://www.ncbi.nlm.nih.gov/pubmed/19457741>](http://ieeexplore.ieee.org/xpls/abs/all.jsp?arnumber=5545378)
- 766 [84] S. Abhyankar, J. Brown, E. M. Constantinescu, D. Ghosh, B. F. Smith, and H. Zhang,
767 “PETSc/TS: A modern scalable ODE/DAE solver library,” *arXiv preprint arXiv:1806.01437*, 2018.
768 <https://arxiv.org/abs/1806.01437>
- 769 [85] R. Weber dos Santos, G. Plank, S. Bauer, and E. J. Vigmond, “Parallel multigrid preconditioner for
770 the cardiac bidomain model.” *IEEE Trans. Biomed. Eng.*, vol. 51, no. 11, pp. 1960–8, nov 2004.
771 doi:[10.1109/TBME.2004.834275](https://doi.org/10.1109/TBME.2004.834275). <http://www.ncbi.nlm.nih.gov/pubmed/15536898>
- 772 [86] G. Plank, M. Liebmann, R. Weber dos Santos, E. J. Vigmond, and G. Haase, “Algebraic multigrid
773 preconditioner for the cardiac bidomain model.” *IEEE Trans. Biomed. Eng.*, vol. 54, no. 4, pp. 585–96, apr
774 2007. doi:[10.1109/TBME.2006.889181](https://doi.org/10.1109/TBME.2006.889181). [http://ieeexplore.ieee.org/lpdocs/epic03/wrapper.htm?arnumber=
775 \[4132940\]\(http://ieeexplore.ieee.org/lpdocs/epic03/wrapper.htm?arnumber=4132940\)\[http://ieeexplore.ieee.org/lpdocs/epic03/wrapper.htm?arnumber=
776 \\[87\\] A. Neic, M. Liebmann, E. Hoetzl, L. Mitchell, E. J. Vigmond, G. Haase, and G. Plank, “Accelerating cardiac
777 bidomain simulations using graphics processing units.” *IEEE Trans. Biomed. Eng.*, vol. 59, no. 8, pp.
778 2281–90, aug 2012. doi:\\[10.1109/TBME.2012.2202661\\]\\(https://doi.org/10.1109/TBME.2012.2202661\\). <http://www.ncbi.nlm.nih.gov/pubmed/22692867>\]\(http://ieeexplore.ieee.org/lpdocs/epic03/wrapper.htm?arnumber=4132940\)](http://ieeexplore.ieee.org/lpdocs/epic03/wrapper.htm?arnumber=4132940)
- 779 [88] E. J. Vigmond, P. M. Boyle, L. Leon, and G. Plank, “Near-real-time simulations of bioelectric activity
780 in small mammalian hearts using graphical processing units.” *Conf. Proc. ... Annu. Int. Conf. IEEE*
781 *Eng. Med. Biol. Soc. IEEE Eng. Med. Biol. Soc. Annu. Conf.*, vol. 2009, pp. 3290–3, jan 2009.
782 doi:[10.1109/IEMBS.2009.5333738](https://doi.org/10.1109/IEMBS.2009.5333738). <http://www.ncbi.nlm.nih.gov/pubmed/3977140>
783 <http://www.ncbi.nlm.nih.gov/pubmed/3977140>
784 {&}tool=pmcentrez{&}rendertype=abstract

- 784 [89] G. Plank, L. Zhou, J. L. Greenstein, S. Cortassa, R. L. Winslow, B. O'Rourke, and N. A. Trayanova,
785 "From mitochondrial ion channels to arrhythmias in the heart: computational techniques to bridge the
786 spatio-temporal scales." *Philos. Trans. A. Math. Phys. Eng. Sci.*, vol. 366, no. 1879, pp. 3381–409, sep
787 2008. doi:[10.1098/rsta.2008.0112](https://doi.org/10.1098/rsta.2008.0112). <http://www.pubmedcentral.nih.gov/articlerender.fcgi?artid=2778066>
788 [http://www.pubmedcentral.nih.gov/articlerender.fcgi?artid=2778066](http://www.pubmedcentral.nih.gov/articlerender.fcgi?artid=2778066&tool=pmcentrez&rendertype=abstract)
[http://www.pubmedcentral.nih.gov/articlerender.fcgi?artid=2778066](http://www.pubmedcentral.nih.gov/articlerender.fcgi?artid=2778066&tool=pmcentrez&rendertype=abstract)
- 789 [90] A. C. Hindmarsh, P. N. Brown, K. E. Grant, S. L. Lee, R. Serban, D. E. Shumaker, and C. S. Woodward,
790 "Sundials: Suite of nonlinear and differential/algebraic equation solvers," *ACM Trans. Math. Softw.*, vol. 31,
791 no. 3, p. 363–396, Sep. 2005. doi:[10.1145/1089014.1089020](https://doi.org/10.1145/1089014.1089020)
- 792 [91] openCARP consortium, C. Augustin, J. Bayer *et al.*, "opencarp (v5.0)," 2021. doi:[10.35097/389](https://doi.org/10.35097/389)
- 793 [92] A. Loewe, G. Seemann, E. M. Wülfers, Y.-L. Huang, J. Sanchez, F. Bach, R. Ulrich, and M. Selzer,
794 "SuLMaSS - sustainable lifecycle management for scientific software," in *E-Science-Tage 2019: Data to*
795 *Knowledge*, Heidelberg, 7 2019. doi:[10.11588/heidok.00026843](https://doi.org/10.11588/heidok.00026843)
- 796 [93] DataCite Metadata Working Group, "Datacite metadata schema documentation for the publication and
797 citation of research data v4.3," 2019. doi:[10.14454/7XQ3-ZF69](https://doi.org/10.14454/7XQ3-ZF69)
- 798 [94] U. Ayachit, *The paraview guide: a parallel visualization application*. Kitware, Inc., 2015.
- 799 [95] J. Bayer, A. J. Prassl, A. Pashaei, J. F. Gomez, A. Frontera, A. Neic, G. Plank, and E. J. Vigmond, "Universal
800 ventricular coordinates: A generic framework for describing position within the heart and transferring data,"
801 *Medical Image Analysis*, vol. 45, pp. 83 – 93, 2018. doi:[10.1016/j.media.2018.01.005](https://doi.org/10.1016/j.media.2018.01.005)
- 802 [96] C. H. Roney, A. Pashaei, M. Meo, R. Dubois, P. M. Boyle, N. A. Trayanova, H. Cochet, S. A. Niederer, and
803 E. J. Vigmond, "Universal atrial coordinates applied to visualisation, registration and construction of patient
804 specific meshes," *Med. Image Anal.*, vol. 55, pp. 65–75, 2019. doi:[10.1016/j.media.2019.04.004](https://doi.org/10.1016/j.media.2019.04.004)
- 805 [97] S. Schuler, N. Pilia, D. Potyagaylo, and A. Loewe, "Cobiveco: Consistent biventricular coordinates
806 for precise and intuitive description of position in the heart – with matlab implementation," 2021.
807 <https://arxiv.org/abs/2102.02898>
- 808 [98] M. Courtemanche, R. J. Ramirez, and S. Nattel, "Ionic mechanisms underlying human atrial action potential
809 properties: insights from a mathematical model," *The American journal of physiology*, vol. 275, no. 1 Pt 2,
810 pp. H301–21, 7 1998. doi:[10.1152/ajpheart.1998.275.1.H301](https://doi.org/10.1152/ajpheart.1998.275.1.H301)
- 811 [99] J. T. Koivumäki, T. Korhonen, and P. Tavi, "Impact of sarcoplasmic reticulum calcium release on cal-
812 cium dynamics and action potential morphology in human atrial myocytes: a computational study." *PLoS*
813 *computational biology*, vol. 7, no. 1, p. e1001067, 1 2011. doi:[10.1371/journal.pcbi.1001067](https://doi.org/10.1371/journal.pcbi.1001067)
- 814 [100] K. H. W. J. ten Tusscher and A. V. Panfilov, "Alternans and spiral breakup in a human ventricular tissue
815 model," *American Journal of Physiology. Heart and Circulatory Physiology*, vol. 291, no. 3, pp. H1088–100,
816 1 2006. doi:[10.1152/ajpheart.00109.2006](https://doi.org/10.1152/ajpheart.00109.2006)
- 817 [101] T. O'Hara, L. Virag, A. Varro, and Y. Rudy, "Simulation of the undiseased human cardiac ventricular action
818 potential: model formulation and experimental validation," *PLoS Computational Biology*, vol. 7, no. 5, p.
819 e1002061, 1 2011. doi:[10.1371/journal.pcbi.1002061](https://doi.org/10.1371/journal.pcbi.1002061)
- 820 [102] A. Loewe, M. Wilhelms, O. Dössel, and G. Seemann, "Influence of chronic atrial fibrillation induced remodel-
821 ing in a computational electrophysiological model," *Biomedizinische Technik / Biomedical Engineering*,
822 vol. 59, no. S1, pp. S929–S932, 2014. doi:[10.1515/bmt-2014-5012](https://doi.org/10.1515/bmt-2014-5012)
- 823 [103] M. Clerx, P. Collins, E. de Lange, and P. G. A. Volders, "Myokit: A simple interface to cardiac cellular
824 electrophysiology," *Progress in Biophysics and Molecular Biology*, vol. 120, no. 1-3, pp. 100–114, 1 2016.
825 doi:[10.1016/j.pbiomolbio.2015.12.008](https://doi.org/10.1016/j.pbiomolbio.2015.12.008)
- 826 [104] C. Mendonca Costa, E. Hoetzel, B. Martins Rocha, A. J. Prassl, and G. Plank, "Automatic parameterization
827 strategy for cardiac electrophysiology simulations," *Comput. Cardiol. (2010)*, vol. 40, no. 2010, pp. 373–
828 376, 2013.
- 829 [105] D. U. J. Keller, D. L. Weiss, O. Dössel, and G. Seemann, "Influence of I(Ks) heterogeneities on the genesis
830 of the t-wave: a computational evaluation," *IEEE Trans. Biomed. Engineering*, vol. 59, pp. 311–322, 2012.
831 doi:[10.1109/TBME.2011.2168397](https://doi.org/10.1109/TBME.2011.2168397)
- 832 [106] S. A. Niederer, Y. Aboelkassem, C. D. Cantwell *et al.*, "Creation and application of virtual patient cohorts
833 of heart models: Virtual Cohorts of Heart Models," *Philos. Trans. R. Soc. A Math. Phys. Eng. Sci.*, vol. 378,
834 no. 2173, 2020. doi:[10.1098/rsta.2019.0558](https://doi.org/10.1098/rsta.2019.0558)

- 835 [107] J. D. Bayer, R. C. Blake, G. Plank, and N. A. Trayanova, “A novel rule-based algorithm for assigning
836 myocardial fiber orientation to computational heart models,” *Annals of Biomedical Engineering*, vol. 40,
837 no. 10, pp. 2243–2254, 1 2012. doi:[10.1007/s10439-012-0593-5](https://doi.org/10.1007/s10439-012-0593-5)
- 838 [108] K. Gillette, J. Bouyssier, M. Gsell, A. Prassl, A. Neic, E. Vigmond, and G. Plank, “Automated Framework
839 for the Inclusion of a Purkinje System in Cardiac Digital Twins of Ventricular Electrophysiology,” *Ann.*
840 *Biomed. Eng.*, under review.
- 841 [109] K. Gillette, M. Gsell, A. Prassl *et al.*, “A Framework for the Generation of Digital Twins of Cardiac
842 Electrophysiology from Clinical 12-leads ECGs,” *Med. Imag. Anal.*, 2021. doi:[10.1016/j.media.2021.102080](https://doi.org/10.1016/j.media.2021.102080)
- 843 [110] S. Schuler and A. Loewe, “Biventricular statistical shape model of the human heart adapted for computer
844 simulations,” Jan. 2021. doi:[10.5281/zenodo.4419784](https://doi.org/10.5281/zenodo.4419784)
- 845 [111] C. Nagel, S. Schuler, O. Dössel, and A. Loewe, “A Bi-atrial Statistical Shape Model and 100 Volumetric
846 Anatomical Models of the Atria,” Dec. 2020. doi:[10.5281/zenodo.4309958](https://doi.org/10.5281/zenodo.4309958)
- 847 [112] S. Pezzuto, P. Kal'avský, M. Potse, F. W. Prinzen, A. Auricchio, and R. Krause, “Evaluation of a
848 rapid anisotropic model for ECG simulation,” *Frontiers in Physiology*, vol. 8, p. 265, May 2017.
849 doi:[10.3389/fphys.2017.00265](https://doi.org/10.3389/fphys.2017.00265)
- 850 [113] T. E. Fastl, C. Tobon-Gomez, A. Crozier *et al.*, “Personalized computational modeling of left atrial ge-
851 ometry and transmural myofiber architecture,” *Medical Image Analysis*, vol. 47, pp. 180 – 190, 2018.
852 doi:[10.1016/j.media.2018.04.001](https://doi.org/10.1016/j.media.2018.04.001)
- 853 [114] A. Wachter, A. Loewe, M. W. Krueger, O. Dössel, and G. Seemann, “Mesh structure-independent modeling
854 of patient-specific atrial fiber orientation,” *Current Directions in Biomedical Engineering*, vol. 1, no. 1, pp.
855 409–412, 1 2015. doi:[10.1515/cdbme-2015-0099](https://doi.org/10.1515/cdbme-2015-0099)
- 856 [115] A. Wachter and A. Loewe, “Resilient,” 2021. doi:[10.5281/ZENODO.4738369](https://doi.org/10.5281/ZENODO.4738369)
- 857 [116] R. Piersanti, P. C. Africa, M. Fedele, C. Vergara, L. Dedè, A. F. Corno, and A. Quarteroni, “Modeling
858 cardiac muscle fibers in ventricular and atrial electrophysiology simulations,” *Computer Methods in Applied*
859 *Mechanics and Engineering*, vol. 373, p. 113468, 1 2021. doi:[10.1016/j.cma.2020.113468](https://doi.org/10.1016/j.cma.2020.113468)
- 860 [117] G. Seemann, C. Höper, F. B. Sachse, O. Dössel, A. V. Holden, and H. Zhang, “Heterogeneous three-
861 dimensional anatomical and electrophysiological model of human atria,” *Philos Trans A Math Phys Eng*
862 *Sci.*, vol. 364, no. 1843, pp. 1465–1481, 1 2006. doi:[10.1098/rsta.2006.1781](https://doi.org/10.1098/rsta.2006.1781)
- 863 [118] C. Corrado, S. Williams, R. Karim, G. Plank, M. O’Neill, and S. Niederer, “A work flow to build and validate
864 patient specific left atrium electrophysiology models from catheter measurements,” *Medical Image Analysis*,
865 vol. 47, pp. 153 – 163, 2018. doi:[10.1016/j.media.2018.04.005](https://doi.org/10.1016/j.media.2018.04.005)
- 866 [119] P. M. Boyle, T. Zghaib, S. Zahid *et al.*, “Computationally guided personalized targeted ablation of persistent
867 atrial fibrillation.” *Nature biomedical engineering*, 8 2019. doi:[10.1038/s41551-019-0437-9](https://doi.org/10.1038/s41551-019-0437-9)
- 868 [120] K. Gillette, A. Prassl, A. Neic, G. Plank, J. Bayer, and E. Vigmond, “Automatic generation of bi-ventricular
869 models of cardiac electrophysiology for patient specific personalization using non-invasive recordings,” in
870 *2018 Computing in Cardiology Conference (CinC)*, vol. 45, 2018, pp. 1–4. doi:[10.22489/CinC.2018.265](https://doi.org/10.22489/CinC.2018.265)
- 871 [121] W. Kahlmann, E. Poremba, D. Potyagaylo, O. Dössel, and A. Loewe, “Modelling of patient-specific purkinje
872 activation based on measured ECGs,” in *Current Directions in Biomedical Engineering*, vol. 3, no. 2. de
873 Gruyter, 1 2017, pp. 171–174. doi:[10.1515/cdbme-2017-0177](https://doi.org/10.1515/cdbme-2017-0177)
- 874 [122] C. H. Roney, A. Pashaei, M. Meo, R. Dubois, P. M. Boyle, N. A. Trayanova, H. Cochet, S. A. Niederer, and
875 E. J. Vigmond, “Universal atrial coordinates applied to visualisation, registration and construction of patient
876 specific meshes,” *Medical Image Analysis*, vol. 55, pp. 65 – 75, 2019. doi:[10.1016/j.media.2019.04.004](https://doi.org/10.1016/j.media.2019.04.004)
- 877 [123] L. Azzolin, S. Schuler, O. Dössel, and A. Loewe, “A reproducible protocol to assess arrhythmia vulnerability
878 in silico: Pacing at the end of the effective refractory period,” *Frontiers in Physiology*, pp. under review,
879 medRxiv preprint available, 2021. doi:[10.1101/2021.01.21.21250205](https://doi.org/10.1101/2021.01.21.21250205)
- 880 [124] M. J. Bishop and G. Plank, “Simulating photon scattering effects in structurally detailed ventricular
881 models using a Monte Carlo approach,” *Front. Physiol.*, vol. 5, no. September, pp. 1–14, sep 2014.
882 doi:[10.3389/fphys.2014.00338](https://doi.org/10.3389/fphys.2014.00338)
- 883 [125] ———, “Biophotonic modelling of cardiac optical imaging,” vol. 859, pp. 367–404, 2015. doi:[10.1007/978-3-319-17641-3_15](https://doi.org/10.1007/978-3-319-17641-3_15)
884

- 885 [126] D. Frisch, T. G. Oesterlein, L. A. Unger, G. Lenis, R. Wakili, C. Schmitt, A. Luik, O. Doessel, and A. Loewe,
886 “Mapping and removing the ventricular far field component in unipolar atrial electrograms.” *IEEE Transac-*
887 *tions on Biomedical Engineering*, vol. 67, no. 10, pp. 2905–2915, 2 2020. doi:[10.1109/TBME.2020.2973471](https://doi.org/10.1109/TBME.2020.2973471)
- 888 [127] M. J. Bishop, E. Vigmond, and G. Plank, “Cardiac bidomain bath-loading effects during arrhyth-
- 889 mias: Interaction with anatomical heterogeneity,” *Biophys. J.*, vol. 101, no. 12, pp. 2871–2881, 2011.
890 doi:[10.1016/j.bpj.2011.10.052](https://doi.org/10.1016/j.bpj.2011.10.052)
- 891 [128] M. J. Bishop and G. Plank, “Bidomain ECG simulations using an augmented monodomain model
892 for the cardiac source.” *IEEE transactions on bio-medical engineering*, vol. 58, no. 8, 8 2011.
893 doi:[10.1109/TBME.2011.2148718](https://doi.org/10.1109/TBME.2011.2148718)
- 894 [129] —, “Representing cardiac bidomain bath-loading effects by an augmented monodomain approach: Ap-
895 plication to complex ventricular models,” *IEEE Trans. Biomed. Eng.*, vol. 58, no. 4, pp. 1066–1075, 2011.
896 doi:[10.1109/TBME.2010.2096425](https://doi.org/10.1109/TBME.2010.2096425)
- 897 [130] A.-M. Plancke, A. Connolly, P. M. Gemmell *et al.*, “Generation of a cohort of whole-torso cardiac models
898 for assessing the utility of a novel computed shock vector efficiency metric for ICD optimisation.” *Comput.*
899 *Biol. Med.*, vol. 112, p. 103368, 2019. doi:[10.1016/j.compbimed.2019.103368](https://doi.org/10.1016/j.compbimed.2019.103368)
- 900 [131] J. Sánchez, M. Nothstein, A. Neic *et al.*, “openCARP: An open sustainable framework for in-silico cardiac
901 electrophysiology research,” in *Computing in Cardiology Conference (CinC)*, ser. Computing in Cardiology
902 Conference (CinC), vol. 47, 1 2020. doi:[10.22489/CinC.2020.111](https://doi.org/10.22489/CinC.2020.111)
- 903 [132] M. D. Wilkinson, M. Dumontier, I. J. J. Aalbersberg *et al.*, “The FAIR guiding principles for scientific data
904 management and stewardship.” *Scientific data*, vol. 3, p. 160018, 3 2016. doi:[10.1038/sdata.2016.18](https://doi.org/10.1038/sdata.2016.18)
- 905 [133] F. Bach, K. Soltau, and M. Razum, “Bedarfsgerechte weiterentwicklung von radar als forschungsdaten-
906 reposititorium für das kit,” in *E-Science-Tage 2019: Data to Knowledge*, V. Heuveline, F. Gebhart, and N. Mo-
907 hammadianbisheh, Eds. University Library Heidelberg, 2019, pp. 162–172. doi:[10.11588/HEIBOOKS.598](https://doi.org/10.11588/HEIBOOKS.598)
- 908 [134] B. F. Lavoie, “The open archival information system reference model: Introductory guide,” *Microform &*
909 *imaging review*, vol. 33, no. 2, pp. 68–81, 2004. doi:[10.1515/MFIR.2004.68](https://doi.org/10.1515/MFIR.2004.68)
- 910 [135] H. Pampel, P. Vierkant, F. Scholze, R. Bertelmann, M. Kindling, J. Klump, H.-J. Goebelbecker, J. Gundlach,
911 P. Schirnbacher, and U. Dierolf, “Making research data repositories visible: The re3data.org registry,” *PLOS*
912 *ONE*, vol. 8, no. 11, pp. 1–10, 11 2013. doi:[10.1371/journal.pone.0078080](https://doi.org/10.1371/journal.pone.0078080)